Developmental Biology 377 (2013) 428–448

Contents lists available at SciVerse ScienceDirect

Developmental Biology

journal homepage: www.elsevier.com/locate/developmentalbiology

Evolution of Developmental Control Mechanisms

Pattern and polarity in the development and evolution of the gnathostome jaw: Both conservation and heterotopy in the branchial arches of the shark, *Scyliorhinus canicula*

Claudia Compagnucci [a,1], Melanie Debiais-Thibaud [b,2], Marion Coolen [c,3], Jennifer Fish [a,d], John N. Griffin [a], Federica Bertocchini [e], Maryline Minoux [f,g], Filippo M. Rijli [f,h], Véronique Borday-Birraux [b], Didier Casane [b], Sylvie Mazan [c], Michael J. Depew [a,i,*]

[a] Department of Craniofacial Development, King's College London, Floor 27, Guy's Hospital, London Bridge, London SE1 9RT, UK
[b] Laboratoire Evolution, Génomes et Spéciation, CNRS and Université Paris Diderot, Paris, France
[c] Development and Evolution of Vertebrates Group, CNRS, Université d'Orléans, UMR 6218, 45070 Orléans, France
[d] Department of Orthopaedic Surgery, UCSF, 513 Parnassus Avenue, Medical Sciences Bldg. S-1161, San Francisco, CA 94143, USA
[e] Instituto de Biomedicina y Biotecnología de Cantabria, Universidad de Cantabria-CSIC-SODERCAN, C. Herrera Oria s/n, 39011 Santander, Spain
[f] Friedrich Miescher Institute for Biomedical Research, Maulbeerstrasse 66, 4058 Basel, Switzerland
[g] Faculté de Chirurgie Dentaire, 1, Place de l'Hôpital, 67000 Strasbourg, France
[h] University of Basel, 4058 Basel, Switzerland
[i] Department of Orthopaedic Surgery, UCSF, 2550 24th Street, SFGH Bldg 9, Room 346, San Francisco, CA 94110, USA

ARTICLE INFO

Article history:
Received 6 October 2012
Received in revised form
26 January 2013
Accepted 18 February 2013
Available online 7 March 2013

Keywords:
Shark
Branchial arch
Heterotopy
Jaws
Evolution

ABSTRACT

The acquisition of jaws constitutes a landmark event in vertebrate evolution, one that in large part potentiated their success and diversification. Jaw development and patterning involves an intricate spatiotemporal series of reciprocal inductive and responsive interactions between the cephalic epithelia and the cranial neural crest (CNC) and cephalic mesodermal mesenchyme. The coordinated regulation of these interactions is critical for both the ontogenetic registration of the jaws and the evolutionary elaboration of variable jaw morphologies and designs. Current models of jaw development and evolution have been built on molecular and cellular evidence gathered mostly in amniotes such as mice, chicks and humans, and augmented by a much smaller body of work on the zebrafish. These have been partnered by essential work attempting to understand the origins of jaws that has focused on the jawless lamprey. Chondrichthyans (cartilaginous fish) are the most distant group to amniotes within extant gnathostomes, and comprise the crucial clade uniting amniotes and agnathans; yet despite their critical phylogenetic position, evidence of the molecular and cellular underpinnings of jaw development in chondrichthyans is still lacking. Recent advances in genome and molecular developmental biology of the lesser spotted dogfish shark, *Scyliorhinus canicula*, make it ideal for the molecular study of chondrichthyan jaw development. Here, following the 'Hinge and Caps' model of jaw development, we have investigated evidence of heterotopic (relative changes in position) and heterochronic (relative changes in timing) shifts in gene expression, relative to amniotes, in the jaw primordia of *S. canicula* embryos. We demonstrate the presence of clear proximo-distal polarity in gene expression patterns in the shark embryo, thus establishing a baseline molecular baüplan for branchial arch-derived jaw development and further validating the utility of the 'Hinge and Caps' model in comparative studies of jaw development and evolution. Moreover, we correlate gene expression patterns with the absence

* Corresponding author at: Department of Orthopaedic Surgery, UCSF, 2550 24th Street, SFGH Bldg 9, Room 346, San Francisco, CA 94110, USA. Fax: +1 415 647 3733.
E-mail address: michael.j.depew@gmail.com (M.J. Depew).
[1] Present Address: Department of Biomedicine, University of Rome "Tor Vergata," 00133 Rome, Italy and Laboratory of Neuroembryology, Fondazione Santa Lucia IRCCS, 00143 Rome, Italy.
[2] Present Address: Institut des Sciences de l'Evolution, Université de Montpellier II, UMR5554, Montpellier Cedex, France.
[3] Present Address: Experimental and Molecular Immunology and Neurogenetics, UMR 7355, Université d'Orleans — CNRS, 45071 ORLEANS, France.

http://dx.doi.org/10.1016/j.ydbio.2013.02.022

of a lambdoidal junction (formed where the maxillary first arch meets the frontonasal processes) in chondrichthyans, further highlighting the importance of this region for the development and evolution of jaw structure in advanced gnathostomes.

Introduction

Vertebrate evolution was profoundly affected by developmental innovations, many – such as the elaboration of the brain, neural crest cells and ectodermal placodes – involving the head (Gans and Northcutt, 1983; Langille and Hall, 1989; Shimeld and Holland, 2000). One result of these innovations, the gnathostome (jawed vertebrate) skull, is structurally complex. Adaptations involving the gnathostome skull have been involved in nearly every major vertebrate transition: in particular, the advent of a segmented, iterated branchial arch skeleton associated with the head enabled the eventual acquisition of jaws among a group of vertebrates—a landmark event that, in large part, lead to an immense gnathostome radiation and diversification (Fig. 1) (de Beer, 1985; Carroll, 1988; Gregory, 1933; Hanken and Thorogood, 1993; Janvier, 1996; Jarvik, 1980; Jollie, 1962; Mallatt, 1997; Radinsky, 1987; Romer, 1966; 1967). In particular, developmental innovations involving the jaws and their primordia have been connected with major evolutionary transitions, including the colonization of land by tetrapods (being in part enabled by acquisition of internal choanae) and the mammalian ability to masticate while breathing (enabled by the presence of a secondary palate) (Carroll, 1992; Evans, 2003; Gans, 1988; Goodrich, 1958; Halstead, 1968; Hildebrand, 1988; Kemp, 2005; Kingsley, 1912; Moore, 1981; Panchen, 1967; Parrington, 1940; Rosen et al., 1981; Schmalhausen, 1968; Tamarin, 1982; Zhu and Ahlberg, 2004).

As a result of this great diversification and radiation, gnathostome skulls (including their jaws) are characterized by variegated elaborations of cranial design that have manifested amazing end-point phenotypes; however, regardless of the particulars of end-point phenotype, gnathostome cranial skeletal ontogeny also notably exhibits a high degree of fidelity to an initial, basic structural design, or baüplan (Allin and Hopson, 1992; Barghusen and Hopson, 1979; de Beer, 1926, 1931, 1985; Bellairs and Kamal, 1981; Cubbage and Mabee, 1996; Depew and Simpson, 2006; Goodrich, 1958; Hanken and Hall,1993; Harrison, 1996; Janvier, 1993; Jarvik, 1980; Jollie, 1957, 1962, 1971; Moore, 1981; Nelsen, 1953; Novacek, 1993; Reynolds, 1913; Rieppel, 1993; Romanoff, 1960; Romer, 1967; Schultze, 1993; Smith, 1993; Trueb, 1993; Watson, 1926; Zusi, 1993). This baüplan includes a chondrocranium composed of a number of basic though fundamental neurocranial and splanchnocranial units, containing the palatoquadrate (PQ) and Meckel's cartilage (MC) cores of the upper and lower jaws, respectively, as well as an associated dermatocranium (in all but chondrichthyans) (Fig. 2). That both structural fidelity and elaboration of end-point phenotypes characterize gnathostome cranial structural organization has led to a number of questions regarding how the genetic, molecular, and cellular mechanisms underlying this apparent fidelity and elaboration of design are (and have been) manifested, maintained, coordinated and modified to generate the known cranial skeletal morphologies.

We have chosen to address such questions by first focusing on the comparative development of gnathostome jaws, initially by asking whether all jaws are made (and patterned) in the same manner. To this end, we have operationally defined and characterized primary jaws as articulated, appositional oral apparatuses principally derived from the splanchnocranial, dermatocranial and associated dental elements arising in the embryo from the anterior most branchial arch (BA), or BA1, with a small yet significant

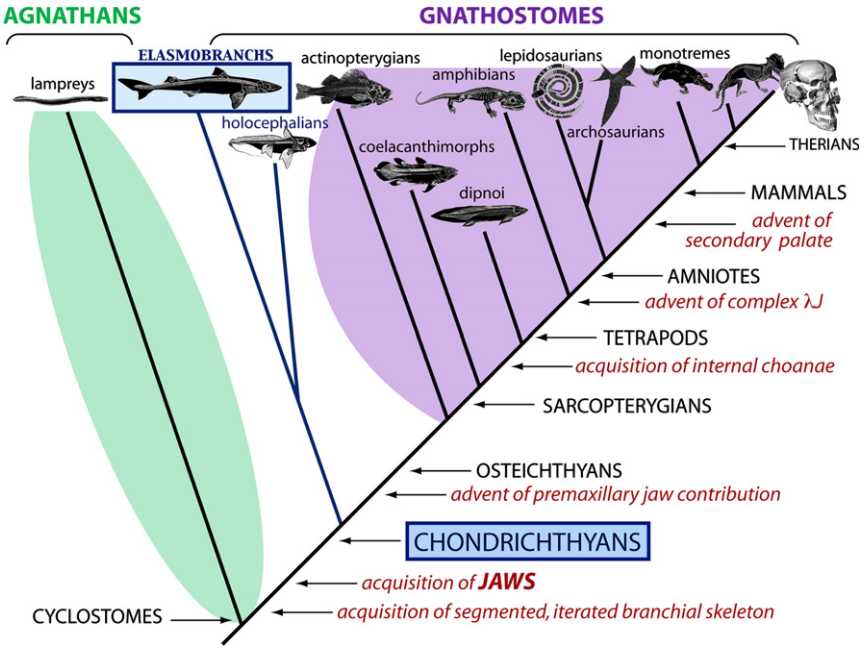

Fig. 1. Vertebrate cladogram emphasizing specific character states in the evolution of jaws. On the cladogram, agnathans such as the lamprey are highlighted in green, chondrichthyans in blue, and osteichthyans (including bony fish and tetrapods) in purple. The lesser spotted dogfish shark, *Scyliorhinus canicula*, is an elasmobranch (boxed in blue) chondrichthyan fish. The acquisitions of specific significant jaw-related character states are indicated in red.

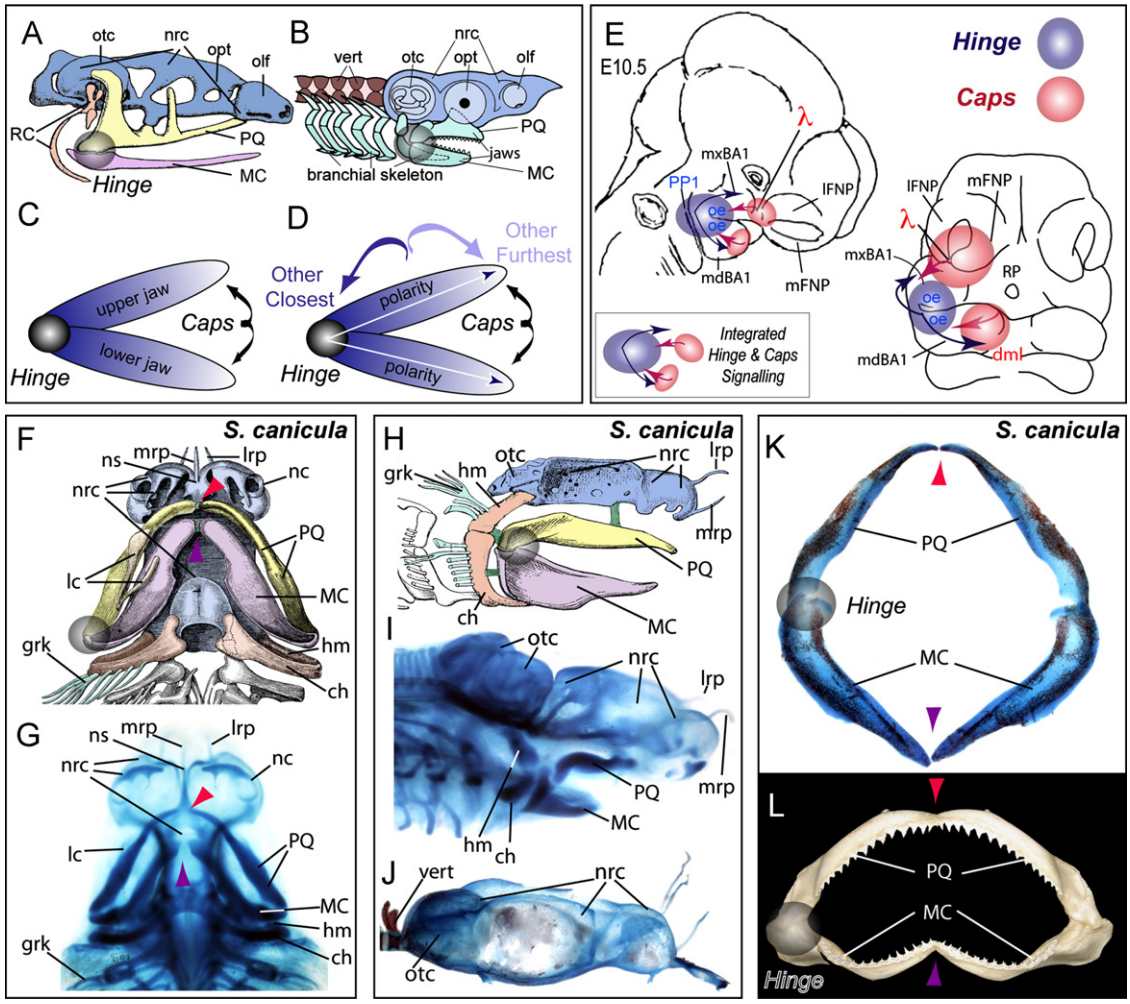

Fig. 2. Jaw pattern and polarity and the adherence of *S. canicula* embryos to the general gnathostome cranial baüplan. (A) Generalized gnathostome chondrocranium. The neurocranium (nrc) is in blue, the palatoquadrate cartilage (PQ) of the upper jaw is in yellow, and Meckel's cartilage (MC) is in lavender. The position of the jaw articulation, or hinge, indicated by the grey disc. (B) Schema of the elasmobranch cranial baüplan. (C) Stylized schema of structural organization of jaws emphasizing the positioning of the hinge (grey disc). (D) Jaw structural polarity relative to the Hinge and the Caps (as representing points furthest from the hinge). (E) Diagram of the integrated nature of the patterning system for developing jaws in amniote embryos, exemplified by the E10.5 mouse, as suggested by the 'Hinge and Caps' model. ((F)–(J)) Classic schemata ((F), (H)) and actual skeletal preparations ((G), (I)–(K)) emphasizing *S. canicula* embryonic cranial organization. The preparation in '(J)' has had its jaws removed. (L) Calcified adult jaws of an elasmobranch shark. The red arrowheads in '(F)', '(G)', '(K)' and '(L)' indicate the PQ elements run medially to articulate with their contralateral, homotypic partners rather than running toward (and articulating with) the laterally placed nasal capsules as is typical for other gnathostomes, while the purple arrowheads indicate the midline meeting of contralateral MC. *Abbreviations*: ch, ceratohyal cartilage; dml, distal mandibular midline; grk, gill raker; hm, hyomandibular cartilage; lc, labial cartilage; lFNP, lateral frontonasal process; lrp, lateral rostral process; MC, Meckel's cartilage; mdBA1, mandibular first branchial arch; mFNP, medial frontonasal process; mrp, medial rostral process; mxBA1, maxillary first branchial arch; nc, nasal capsule; nrc, neurocranium; ns, nasal septum; oe, oral ectoderm; olf, olfactory capsule; opt, optic capsule; otc, otic capsule; PP1, first pharyngeal plate; pq, palatoquadrate; RC, Reichert's cartilage; RP, Rathke's pouch; vert, vertebrae; λ, lambdoidal junction.

contribution, in all but chondrichthyans, from the olfactory placode-associated frontonasal prominences (FNP). Thus defined, polarity is an inherent character state of jaws as minimally there is the 'Hinge' and there is all 'Other' (i.e., everything else) (Fig. 2). A significant consequence of such polarity is the potential for modularity within the appositional units (Depew and Compagnuicci, 2008; Fish et al., 2011). Modularity is a notable trait as (1) it plausibly explains both integration within jaw structures and autonomy between jaw structures and (2) it potentially provides a key mechanism for evolutionary modifications and transformations of jaws.

The developmental system that coordinates and patterns the craniofacial primordia that give rise to jaws involves an intricate spatiotemporal series of reciprocal inductive and responsive interactions between the cephalic epithelia (both endodermal and ectodermal) and the cranial neural crest (CNC) and cephalic mesodermal mesenchyme (reviewed in Depew et al., 2002b; Francis-West et al., 2003; Minoux and Rijli, 2010). The coordinated regulation of these interactions is critical for both the ontogenetic registration of the jaws (i.e., yielding appositional units working as a functional whole) and the evolutionary elaboration of variable jaw morphologies and designs. Following the above operational definition of jaws, a 'Hinge and Caps' model has previously been proposed that addresses the mechanisms of jaw development and evolution by placing the articulation, and subsequently the polarity (and potential modularity), of the upper and lower gnathostome jaws in the context of CNC competence to respond to positionally located cephalic epithelial signals (for discussions, see: Depew et al., 2005; Depew and Simpson, 2006; Depew and Compagnuicci, 2008). Like most current models of jaw development and evolution, which have arisen mostly from molecular and cellular data in chicks and mice with some augmentation from other osteichthyan model organisms such as the zebrafish, this model expands on an evolving model of jaw

development and polarity within the amniote BA1. The 'Hinge and Caps' model seeks to explain a developmental patterning system that apparently keeps gnathostome jaws in functional registration yet tractable to potential changes in functional demands over time. More specifically, it relies upon a system for the establishment of positional information where pattern and placement of the 'Hinge' is driven by factors common to the junction of the maxillary (mxBA1) and mandibular (mdBA1) branches of BA1 (including the oral epithelium and the first pharyngeal plate), and of the 'Caps' by the signals emanating from the distal-most BA1 midline and the lambdoidal junction (where mxBA1 meets the FNP; hereafter λ-junction) (Fig. 2). In this particular model, the functional registration of jaws is achieved by the integration of 'Hinge' and 'Caps' signaling, with the 'caps' sharing at some critical level a developmental program that potentiates their own coordination. The model further posits that empirical patterns of regional gene expression at pharyngula stages of gnathostome embryos reflects the 'Hinge and Caps' nature of the patterning system of jaws.

Current models of jaw development and evolution have been built on molecular and cellular evidence gathered mostly in amniotes and partnered by essential work attempting to understand the origins of jaws that has focused on the jawless lamprey (Depew and Simpson, 2006; Myojin et al., 2001; Kuratani, 2004, 2005, 2012; Shigetani et al., 2002). Clearly lacking, however, is any understanding of the molecular and cellular underpinnings of jaw development in chondrichthyans, the gnathostome outgroup to osteichthyans and the clade to be compared to agnathans and osteichthyans in order to infer the ancestral state in the gnathostome last common ancestor (Fig. 1). Chondrichthyans are amongst the oldest, most basal extant gnathostomes making them essential targets of investigations in the analysis of jaw development and evolution (de Beer, 1931; Carroll, 1988; Coolen et al., 2009; Daniel, 1934; Dean, 1909; El-Toubi, 1949; Godard and Mazan, 2012; Goodrich, 1909, 1918; Gregory, 1933; Holmgren, 1940, 1942; Radinsky, 1987; Schaeffer and Williams, 1977; Wilga, 2002). Despite their apparent possession of the oldest, least modified jaws, how similar or different the spatiotemporal expression patterns are in chondrichthyans of genes known to be critical for amniote jaw development is unknown.

The Chondrichthyan clade consists of the *Elasmobranchii* (skates, rays and sharks) and the *Holocephali* (chimaeras) (Fig. 1). Chondrichthyans exhibit fundamental vertebrate characteristics, such as CNC and an adaptive immune system, as well as fundamental gnathostome characteristics such as jaws and teeth (Coolen et al., 2007, 2009; Didier et al., 1998; Ferreiro-Galve et al., 2008; Freitas and Cohn, 2004; Gillis et al., 2009a, 2009b, 2011; Holmgren, 1940, 1942; Kuratani and Horigome, 2000; Maisey, 2001, 2008; Meyer and Zardoya, 2003; Nelsen, 1953; O'Neill et al., 2007; Reif, 1980; Romer, 1966; Smith et al., 2009; Wilga, 2002; Wotton et al., 2008). While in general gnathostomes have, in addition to their splanchnocranial cores, a dermatocranial component to their jaws, elasmobranches such as the shark have much simpler jaw apparatuses: their upper jaws consist of calcified PQ cartilages and associated teeth while their lower jaws consist of calcified MC cartilages and associated teeth (Barghusen and Hopson, 1979; de Beer, 1931; Carroll, 1988; Daniel, 1934; Dean, 1909; El-Toubi, 1947, 1949; Goodrich, 1909, 1918; Gregory, 1933; Grogan et al., 1999; Kingsley, 1912). Significantly, sharks do not possess FNP-premaxillary components in their upper jaws. Due to its phylogenetic position within the chondricthyes, the natural sister group of osteichthyes (bony fish, amphibians, and amniotes), the shark has historically been a significant model organism in comparative anatomy and physiology (Balfour, 1878; de Beer, 1931; Dean, 1909; Daniel, 1934; El-Toubi, 1949; Goodrich, 1918; Holmgren, 1940; Kingsley, 1907; Schultze, 1993). Recent advances in genomic resources as well availability of eggs, make the lesser spotted dogfish shark, *Scyliorhinus canicula*, a significant model organism for the renewed, molecular study of the origins and diversification of jaws (Coolen et al., 2009; Godard and Mazan, 2012). Moreover, *S. canicula*, as a scyliorhinid shark, is a basal member of the largest order of extant sharks, the Carcharhinininiformes, which comprise one of the four groups of Galeomorph chondrichthyans. As such, *S. canicula* is representative of the *Elasmobranchii*, one of the most basal, extant natural groups of gnathostomes (Fig. 1; Arnason et al., 2001; Iglesias et al., 2005). Herein, we further examine the empirical foundation for the 'Hinge and Caps' model by investigating evidence of heterotopic (relative changes in position) and heterochronic (relative changes in timing) shifts in gene expression, relative to amniotes such as mice, in the jaw primordia of *S. canicula*.

Materials and methods

Anatomical analyses

Staining of skeletal tissues of embryos harvested from egg cases was achieved following established protocols, where the Alizarin Red stained calcified cartilage and dermal denticles, while Alcian Blue stained uncalcified cartilaginous tissues (Depew, 2008). Samples were stored in 100% glycerol at room temperature. Skeletal preparations were photographed using a Leica MZFLIII microscope with a Leica DFC300FX camera.

Scanning electron microscopy

Freshly harvested embryos were fixed in 4% paraformaldehyde and 0.2% glutaraldehyde in PBS. The specimens were then washed in PBS, dehydrated in a graded ethanol series, and critical point dried in liquid carbon dioxide. Specimens were subsequently mounted onto aluminum stubs and sputter coated with gold-palladium. They were thereafter examined and photographed with a FEI Quanta FEG scanning electron microscope operating at 10 kV.

Whole embryo in situ hybridization

Digoxygenin-labelled ribroprobes were prepared from cDNA extracted from *S. canicula* embryos and subsequently cloned in pSPORT vectors. Cloned fragments were amplified using the following primers: 5′ cDNA-pSPORT1 (5′AAAGC TGGTACGCCTGCA) and T7-3′pSPORT1 (5′TAATACGACTCACTATAGGGAGAGCGTACG TAAGCTTGGATC). The obtained PCR product was purified using a High Pure kit (Roche). Shark embryos were fixed with 4% paraformaldehyde in PBS over-night at 4°C on a rotating platform. Samples were then rinsed, dehydrated in a MeOH series, and subsequently stored at −20° C in 100% MeOH until use. Whole mount in situ hybridization was performed following Depew et al. (1999).

Results

The embryonic jaws and their branchial arch antecedents in Scyliorhinus canicula

The developing chondrocranium (including the splanchnocranium) of *S. canicula* has historically been used as illustrative of the general elasmobranch chondrichthyan state (Fig. 2B, F and H) (e.g.,

de Beer, 1931). Pre-hatching embryos harvested from egg cases and subsequently stained with alcian blue demonstrate the adherence of *S. canicula* embryos to the general gnathostome baüplan (Fig. 2F–K). The chondrocranium consists of a neurocranium with sensory capsules and a splanchnocranium containing significant PQ and MC elements of the upper and lower jaws, respectively. Two notable differences between the elasmobranch chondrichthyan and osteichthyan jaws are evident: first, elasmobranch jaws such as those of *S. canicula* do not contain a dermatocranium associated with the PQ and MC elements; and second, rather than running toward (and articulating with) the laterally placed nasal capsules, PQ elements run medially to articulate with their contralateral, homotypic partners.

Despite a significant history in anatomical analyses, the jaw-yielding branchial arches of *S. canicula* have rarely been the focus of investigation in and of themselves. To facilitate our comparative analysis of the shark BA, we used scanning electron microscopy, which exquisitely details the surface appearance of anatomic, including embryonic, structures (Tamarin and Boyde, 1977; Tamarin, 1982), to further characterize the BA of *S. canicula* embryos from stage 17 to stage 25 (see Ballard et al., 1993, for staging criteria). Though differential translucence using light microscopy reveals the presence of the first pharyngeal pouch (Ballard et al., 1993), at stages 17 and 18 the external surfaces of the cephalic region of *S. canicula* embryos do not yet evince clearly demarcated individual BA (Fig. 3A and B). From stage 19 onward, however, discernable BA are present, and by stage 21 the anterior pharyngeal plates uniting the pharyngeal clefts with the pharyngeal pouches have begun to rupture between the BA (Fig. 3C). At this stage the BA are dorso-ventrally oriented

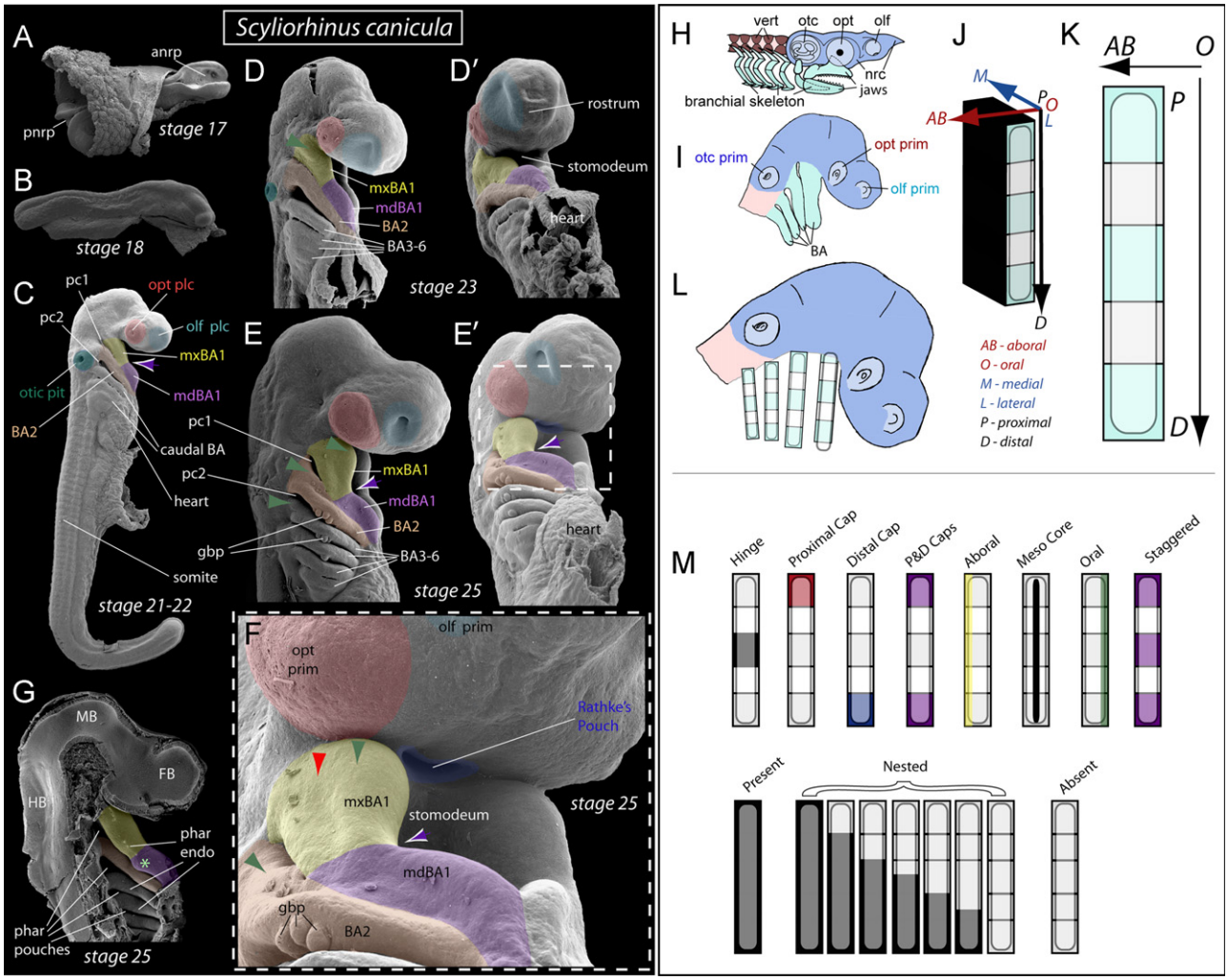

Fig. 3. Characterization of pharyngeal stage *S. canicula* craniofacial primordia. ((A)–(F)) Scanning electron micrographs of stage 17, 18, 21, 23 and 25 *S. canicula* embryos. Various cranial primordia are pseudo-colored to facilitate comparison between stages. White bordered blue arrows indicate the maxillary–mandibular constriction between mxBA1 and mdBA1, while the green and red arrowheads emphasize the distinctive oral (green) and aboral (red) subdivisions of the proximal BA. In the stage 25 embryo (E, E′ and F, where E′ is an oblique view of the embryo in E and F is a magnified view of E′), the close proximity of contralateral mxBA1 to each other and to Rathke's pouch (pseudo-colored blue) at the midline is clearly in evidence. This proximity further emphasizes the great distance, typical of elasmobranchs, between the mxBA1 and the invaginating olfactory pit. The embryo in 'G' is hemi-sected to reveal the pharyngeal endodermal (phar endo) surface of the BA and pharyngeal pouches (phar pouches). The asterisks in 'G' indicates a discrete mandibular bulge. *Pseudocoloring*: red, optic primordia; turquoise, olfactory primordia; salmon, second branchial arch; green, otic pit; yellow, maxillary first branchial arch; lavender, mandibular first branchial arch. ((H)–(L)) Color-coordinated schemata of the jaws (H) and their antecedent BA primordia (in green) in the shark (I). The BA of the shark, typically being proximo-distally elongated structures, are particularly amenable to schematization. For instance, in '(J)' and '(K)' the oral–aboral, medial-lateral and proximal–distal axes of the branchial arches are schematized in three (J) and two (K) dimensions. The green boxes in the schematized BA of '(J)–(L)' are indicative of the notion of modularity as a potential consequence of a 'hinge and caps' system of patterning of the BA. (M) Various anticipated patterns of BA gene expression, as posited by the 'hinge and caps' model, superimposed on two-dimensional schemata of shark BA1. *Abbreviations*: anrp, anterior neuropore; BA, branchial arch; FB, forebrain; gbp, gill bud primordia; HB, hindbrain; MB, midbrain; mdBA1, mandibular first branchial arch; mxBA1, maxillary first branchial arch; nrc, neurocranium; olf, olfactory (nasal) capsule; olf plc, olfactory placode; olf prim, olfactory primordia; opt plc, optic placode; opt prim, optic primordia; otc prim, otic primordia; pc, pharyngeal cleft; pnrp, posterior neuropore; vert, vertebrae.

and rod-like, with BA1 beginning to show the oral maxillary–mandibular constriction (MMC) that characterizes later stage embryos (white and purple arrowheads, Fig. 3). Moreover, otic, optic, and olfactory placodogenesis has occurred and incipient sensory primordia are developing dorsad to the BA (Fig. 3).

By stage 23, the first six BA are delineated, and, while clearly still rod-like in nature, a dorso-lateral (proximal) to ventro-medial (distal) orientation becomes evident. Two significant traits are further apparent at this stage: first, unlike amniote embryos, the proximal (dorsal) ends of each mxBA1 do not run toward olfactory pits but rather run dorsad just caudal to the developing optic primordia (compare Fig. 2E and Fig. 3D); second, an oral (rostral)–aboral (caudal) polarity initially becomes evident, as evinced by discrete bulges within the oral–aboral axes of the individual BA (exemplified by green arrowhead, Fig. 3D).

Further intra-arch polarity is patent by stage 25 (a stage, based on relative cephalic placode and BA development, roughly equivalent to E10-11 in mice) when the proximal end of the first three BA are distinctly comprised of two discrete, proximo-distally oriented, bulges (see green arrowheads, Fig. 3E and F). The MMC is accentuated at this stage, and gill bud primordia have begun to sprout on the caudal (aboral) aspect of BA2–BA4 (Fig. 3E and F). Notably, gill buds appear to sprout from a mid-way point along the BA – proximo-distally aligned with the position of MMC – and appear to proliferate both proximally and distally from this point. The BA, moreover, have taken an overall chevron shape (Fig. 3E′), bent at the position of the constriction and buds, with the distal mandibular ends running toward the midline and heart. The proximal-most mxBA1 of stage 25 embryos, while still beneath the optic primordia, are also strikingly close to Rathke's pouch as they have begun to run toward their contra-lateral, homotypic partners (Fig. 3F), and do not run toward the developing olfactory apparatus. Unlike similarly staged amniote nasal pits, the olfactory invaginations of the shark at this stage are only deep dorsally, creating a round, dorsal frontonasal mass with little evidence of discrete medial and lateral FNP: thus, discrete λ-junctions are not seen. The linguo-caudal aspect of the proximal end of mdBA1, just before the MMC, further exhibits a discrete bulge (green asterisk, Fig. 3G), additionally highlighting the patent morphologic polarity within the *S. canicula* BA.

Thus, by stage 25, the BA of *S. canicula* embryos exhibit clear proximo-distal (dorso-ventral), oral–aboral (rostro-caudal) and medio-lateral (buccal–lingual) morphologic – and therefore developmental – polarity (Fig. 3H–M). This polarity can be schematized with reference to the expectations of gene expression patterns posited in the 'Hinge and Caps' model, and aspects of the developing axes (whether one, two or three dimensional) of the BA can be visualized to facilitate comparisons with osteichthyan (or amniote) embryos. For instance, gene expression may be hinge-centric (i.e., hinge-related), cap-centric, oral-centric, aboral-centric, nested, etc. (Fig. 3M). For convenience, we utilize this ordering mechanism in our analysis, presented below, of gene expression patterns investigated in *S. canicula* embryos.

Gene nesting patterns within the shark BA: The elasmobranch Dlx code

Dlx genes in amniotes are expressed in appendages, or outgrowths, from the main body axis, including in the basal ganglion, limb buds, genital tubercle and BA (Panganiban and Rubenstein, 2002). In amniotes, six *Dlx* genes have been detected and described: *Dlx1*, *Dlx2*, *Dlx3*, *Dlx5*, *Dlx6* and *Dlx4* (reviewed in Depew et al., 2005). In the embryonic mouse, these six *Dlx* genes are differentially expressed in a regional, nested pattern in the ectomesenchyme along the proximo-distal axis of the BA (Fig. 4A–C). Notably, *Dlx* genes are also variably expressed in the cephalic ectoderm. Chromosomal organization is, moreover, believed to be key to *Dlx* biology, with the six genes arranged as tightly linked, convergently transcribed (tail-to-tail), bigene tandems (or first-order (cis) paralogues) located near *Hox* gene clusters (Stock et al., 1996; Panganiban and Rubenstein, 2002). Protein structural similarity outside of the homeodomain, plus chromosomal location, indicates that the *Dlx* genes can be placed into two clades of second-order (trans) paralogous groups: *Dlx1/6/4* and *Dlx2/5/3*. Tightly linked *Dlx* genes share regulatory regions and are expressed in similar patterns within the developing BA mesenchyme (Dolle et al., 1992; Bulfone et al., 1993; Robinson and Mahon, 1994; Ellies et al., 1997a,b; Depew et al., 2002a, Panganiban and Rubenstein, 2002; Ghanem et al., 2003; Qiu et al., 1995, 1997; Sumiyama and Ruddle, 2003). Hence, the linked, first-order paralogous *Dlx* bigenes share nested expression patterns within the mesenchyme of the BAs: the linked pair *Dlx1/2* are expressed throughout mxBA1 and mdBA1 while the *Dlx5/6* pair is essentially restricted to mdBA1 and *Dlx3/4* to a sub-domain therein (Fig. 4A–C).

Based on genetic loss-of-function experiments in mice, and the familial nested expression pattern within the amniote BA ectomesenchyme, it has been argued that a *Dlx* code for regional specification along the proximo-distal axis of the BA regulates intra-BA skeletal morphology (Depew et al., 2002a,b, 2005). This code is in line with the 'Hinge and Caps' model as *Dlx* nesting and morphologic transformations due to loss of nested genes roughly correlate to mxBA1–mdBA1 divisions centered about the presumptive hinge region of BA1. Though stringent spatial and temporal detailing has yet to be presented, *Dlx* nesting in the BA of other osteichthyans, including zebrafish, cichlids and chicks, has generally been in line with what has been published for mice (Blentic et al., 2008; Ellies et al., 1997a, 1997b; Renz et al., 2011; Talbot et al., 2010; Walker et al., 2006) (Fig. 4A–C). Lampreys, which lack segmented branchial structures, possess multiple Dlx genes but, notably, nesting does not appear to characterize expression in their BA (Neidert et al., 2001; Kuraku et al., 2010; Kuratani, 2012; but see also Cerny et al., 2010).

Previous work has demonstrated that chondrichthyans are aligned with amniotes, rather than with teleostean bony fish such as *Danio rerio* which exhibit additional chromosomal duplications followed by loss, in possessing an array of three linked-pairs of *Dlx* genes (Renz et al., 2011; Stock, 2005; Ellies et al., 1997a,b). To determine whether *Dlx* nesting is a shared feature of chondrichthyan and osteichthyan BA development (i.e., is symplesiomorphic), we examined six *S. canicula* genes (*ScDlx1*, *ScDlx2*, *ScDlx3*, *ScDlx4*, *ScDlx5* and *ScDlx6;* Debiais-Thibaud et al., 2011) homologous (orthologous) to amniote *Dlx1-6* and addressed the ontogeny of the patterns of their gene expression in the BA, beginning with the *ScDlx2/5/3* trans paralogous group.

ScDlx2

At stage 19, streams of *ScDlx2+* cells leaving the neural folds and entering the BA are detected through in situ hybridization (blue arrows, Fig. 4F). *ScDlx2+* cells are also detected circling the dorsal aspect of the optic primordia, as well as in two stripes, one connecting the circum-optic population with the midbrain stream entering BA1 (red arrows, Fig. 4F) and another directed, rostral to the eye, dorsad over the forebrain (green arrows, Fig. 4F). At stage 20, *ScDlx2* transcripts clearly fill the entire lengths of the first three BA (yellow arrows), including mxBA1 and mdBA1, and are beginning to fill BA4. By stage 25, *ScDlx2* transcripts are still detectable throughout the proximo-distal axis of BA1–BA6, though the distal (e.g., mdBA1) halves of BA1–BA3 show noticeably less strength of signal. Moreover, at this stage the mid-way position of the BA, aligned with the MMC, evince the weakest levels of transcript (yellow asterisks, Fig. 4F). At

stage 27 this trend toward reduction of expression distally has intensified such that, whilst proximal BA ectomesenchyme remain highly *ScDlx2*-positive, relatively little expression is seen in the distal halves of the BA including mdBA1. Unlike what is seen with murine *Dlx2*, *ScDlx2* transcripts are not detected in the epithelium of the distal mdBA1 midline or at the proximal most mxBA1 at these stages (orange arrows, Fig. 4F).

ScDlx5

ScDlx5 transcripts are initially detected at stage 18 in the midline surface cephalic epithelium associated with the recently closed anterior neuropore (Fig. 4G and Supplementary Fig. 2) and continue to be expressed here through stage 25. *ScDlx5* transcripts are clearly detected in BA1-3 by stage 21, though

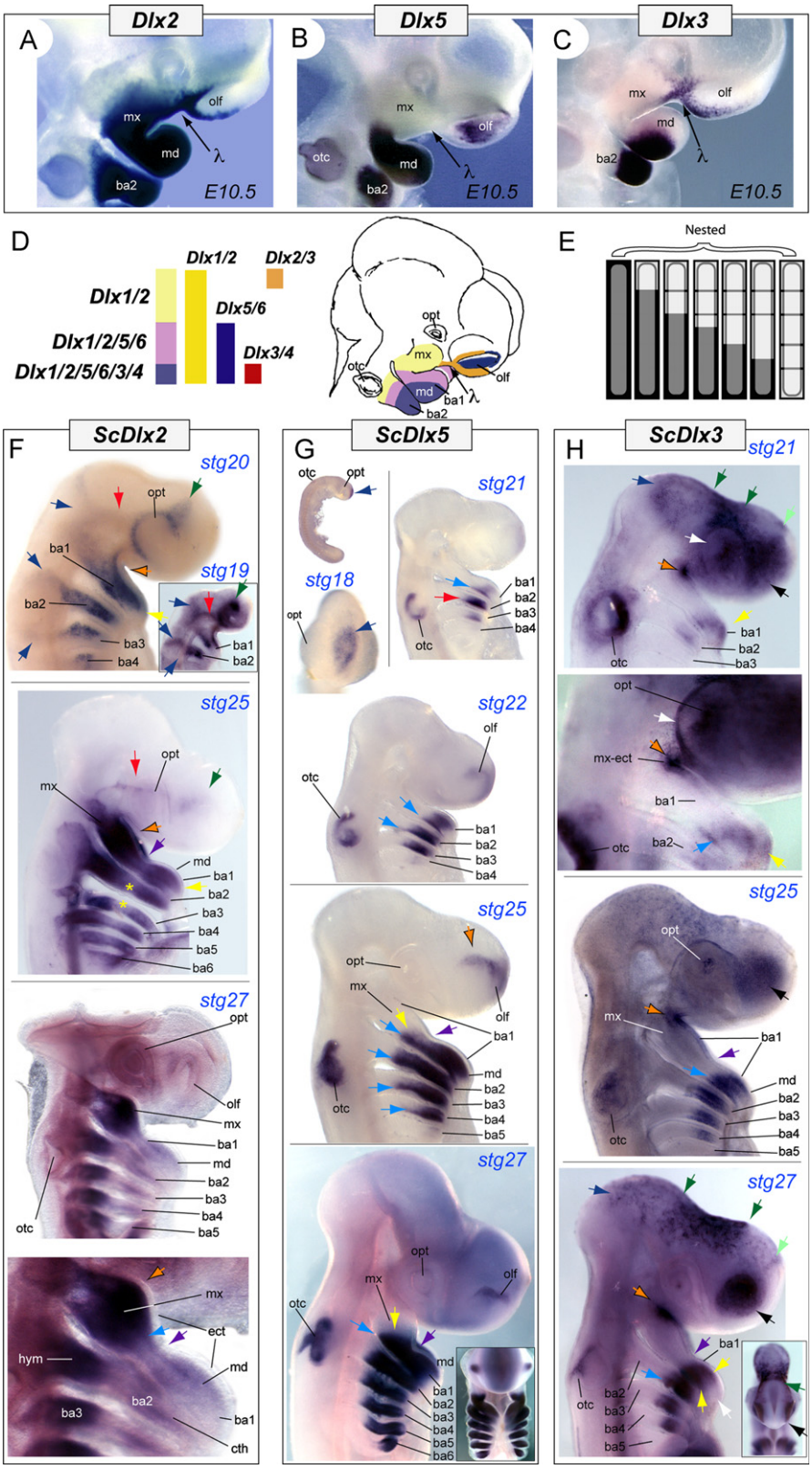

BA2 distinctly appears to have greatest levels at this stage (red arrow, Fig. 4G). Stages 21–22 also highlight a subsequent trend toward an oral–aboral (rostro-caudal) asymmetry of expression in the BA as the aboral edge of ectomesenchymal expression extends proximally further than the oral edge (see light blue arrows, Fig. 4G). An additional trend, seen beginning stage 25, is the extension of significant *ScDlx5* expression (yellow arrows, Fig. 4G) in the BA proximal to the position of the MMC. Moreover, epithelial expression is also detected in the dorsal olfactory placode and pit (orange arrows, Fig. 4G).

ScDlx3

ScDlx3 displays an overall dynamic cephalic embryonic expression pattern, in particular outside of the BA (Fig. 4H). From stage 21 through stage 27, *ScDlx3* expression is seen in the proximal-most oral ectoderm of mxBA1 (orange arrows, Fig. 4H). *ScDxl3* is also detected in the distal BA, coming on simultaneously, or just soon after, *ScDlx5*. Transcripts of *ScDlx3* are clearly nested within the *ScDlx5* domain, but unlike *ScDlx5* do not, at any stage, extend proximally past the MMC. The oral–aboral asymmetry of expression characteristic of *ScDlx5* is likewise evinced, to a lesser degree, with *ScDlx3* in BA1, but is not significant in the caudal BAs. *ScDlx3* is extensively expressed in the ectoderm associated with the primary sensory placodes, most notably in the ectoderm of the olfactory primordia.

ScDlx1, ScDlx4 and ScDlx6

As stated above, *ScDlx1*, *ScDlx4* and *ScDlx6* form linked pairs with *ScDlx2*, *ScDlx3* and *ScDlx5*, respectively. As has typically been seen in osteichthyans, the expression patterns of linked pairs in *S. canicula* generally mirror each other though small differences are encountered (Supplementary Figs. 1 and 2). For instance, *ScDlx6* is expressed in the distal halves of the BA, including mdBA1, but does not extend proximally at later stages as its linked pair gene, *ScDlx5*, does. Overall, *S. canicula* exhibits a tiered, terraced nested pattern of *Dlx* gene family expression.

Conservation of hinge-centric patterns of gene expression

The 'Hinge and Caps' model suggests that the placement of the jaw articulation (i.e., the hinge) is fundamental to the patterning and organization of the jaws (Depew and Simpson, 2006; Depew and Compagnuicci, 2008). Corollary to this notion is the expectation that unique, hinge-centric patterns of gene expression will characterize the antecedent jaw articulation region of the BA. We therefore examined whether *S. canicula* evinced patterns of gene expression similar to amniote genes typically found at the mxBA1–mdBA1 juxtaposition at the hinge (Fig. 5A). Specifically, we examined the expression of *S. canicula* homologues of *Emx1*, *Emx2* and *Bapx1*, three genes expressed at the mxBA1–mdBA1 juxtaposition (i.e., the hinge) in amniotes (Bell et al., 2001; Gorski et al., 2002; Lettice et al., 2001; Mihailescua et al., 1999; Santagati et al., 2005; Tucker et al., 2004; Williams et al., 1997; Fig. 5).

We found that, in addition to being expressed in the brain (Derobert et al., 2002), at stage 25+*ScEmx1* and *ScEmx2* are both expressed in the BA of pharyngula stage *S. canicula* embryos (Fig. 5). Specifically, expression is centered midway along the proximo-distal axis of the BA, positionally aligned with the MMC (Fig. 5B and C). Expression of *ScEmx1* is particularly dynamic in this position (Fig. 5B), with transcripts being detectable orally and aborally at the MMC as well as in a lateral proximo-distal stripe placed midway between the oral and the aboral aspects of BA1 (yellow arrows, Fig. 5B). Moreover, a slight asymmetric oral–aboral expression pattern, still centered midway along the proximo-distal axis, characterizes the caudal BA (Fig. 5B). *ScEmx2* expression (Fig. 5C), much like that seen with murine *Emx2* (Fig. 5D), is highly hinge-centric.

Bapx1 expression in amniotes has been specifically correlated with the PQ–MC articulation (i.e., with the 'primary' jaw articulation; Lettice et al., 2001; Miller et al., 2003; Tucker et al., 2004), and therefore *Bapx1* represents a notable hinge-centric gene (Fig. 5G). In pharyngula stage *S. canicula* embryos from stage 19 to stage 27, *ScBapx1* is hinge-centric, being elaborately expressed around the MMC as well as in positionally aligned cells of the caudal BA (Fig. 5E and F). In particular, at stages 25 and 27, *ScBapx1* transcripts are found in both the endoderm and the ectoderm associated with the pharyngeal clefts, being off-set between the oral (rostral; blue arrows) and aboral (caudal; yellow arrows) aspects of each BA (Fig. 5E and F).

We further considered evidence of either the specific absence, or the relative down-regulation, of gene expression at the MMC (and its positional correlates in the caudal BA) to be further evidence of hinge-related patterns of gene expression. In this regard, we found *ScShh* expression an exemplar of the latter category. Specifically, the extensive *ScShh* expression that characterized the proximo-distal axes of the endodermal linings of the BA from stage 21 to stage 25 was found to be distinctly diminished at the MMC as well as midway along the proximo-distal axes of the more caudal BA (Fig. 5H).

Conservation of caps-centric patterns of gene expression

Finding that *S. canicula* shared with amniote embryos hinge-centric patterns of expression of specific genes, we sought further evidence of shared, conserved (symplesiomorphic) patterns of expression within the 'Caps' regions of shark embryos.

Fig. 4. Patterns of nested *ScDlx* expression in *S. canicula*. ((A)–(C)) Patterns of gene expression of *Dlx2* (A), *Dlx5* (B) and *Dlx3* (C) in E10.5 mouse embryos. (D) Summary schema of nested murine *Dlx* gene expression. (E) Reiterated schema of potential nested patterns in shark BA. ((F)–(H)) *ScDlx* gene expression. (F) *ScDlx2* expression in stage 19, 20, 25 and 27 *S. canicula* embryos. Red arrows indicate a distinct post-optic streak of labeling while the green indicate a pre-optic streak. Blue arrows highlight streams of CNC entering the BA. The purple arrow points to the maxillary–mandibular constriction (MMC). The yellow arrows indicate the distal extension of expression into the mandibular BA1 (md). In the stage 25 panel, yellow asterisks are aligned with the position of the mmc where distal expression first begins to be down regulated. The light blue arrow in the magnified panel of the stage 27 embryo highlights the recession, just proximal to the MMC, of transcript detection into the mxBA1 domain. The black-bordered orange arrow points to the lack of signal in the maxillary ectoderm. (G) *ScDlx5* expression in stage 18, 21, 22, 25 and 27 *S. canicula* embryos. At stage 18, transcripts are detectable in the anterior ectoderm associated with the closing anterior neuropore (dark blue arrows) but not yet in the BA. Expression of *ScDlx5* is subsequently found in the distal BA of stage 21 and 22 embryos. An oral–aboral asymmetry in expression is apparent whereby transcripts extend slightly further proximally in the aboral (caudal) side of the BA (light blue arrows). The purple arrow points to the MMC. The significance of greater expression in ba2 at early stages is unclear (red arrow). Notably, by stage 25, *ScDlx5* transcripts extend beyond the position of the MMC. (H) Dynamic cephalic *ScDlx3* expression in stage 21, 25 and 27 *S. canicula* embryos. Dark blue and green arrows highlight distinct ectomeric boundaries of expression covering the mid- and forebrains of *S. canicula* embryos. The black-bordered orange arrows indicate mxBA1 ectodermal expression, while black arrows indicate the olfactory ectodermal expression. Oral–aboral asymmetry in BA expression of *ScDlx3*, which is distally restricted in general, is also seen (light blue arrows) although it is less than what is seen with *ScDlx5*. Yellow arrows highlight the distal extent of expression in the first arch. *Abbreviations*: ba1–6, branchial arches 1 through 6; cth, ceratohyal branch of the second branchial arch; ect, ectoderm; hym, hyomandibular branch of the second branchial arch; md, mandibular first branchial arch; mx, maxillary first branchial arch; mx-ect, ectoderm of maxillary BA1; olf, olfactory primordia; opt, optic primordia; otc, otic primordia; stg, stage; λ, lambdoidal junction.

Specifically, we examined three subtypes of gene expression: (1) genes dually expressed in both the proximal BA1 associated with the amniote λ-junction and the distal mdBA1, including *Prx1*, *Alx4*, *Tbx2* and *Bmp4* (Fig. 6; Ashique et al., 2002; Barlow and Francis-West, 1997; Bei and Mass, 1998; ten Berge et al., 1998; Beverdam et al., 2001; Foppiano et al., 2007; Furuta and Hogan, 1998; Chesterman and Kern, 2002; Depew et al., 2002b; Francis-West et al., 2003; Gong and Guo, 2003; Liu et al., 2005a, b; McGonnell et al., 2011; Qu et al., 1998, 1999; Satokata and Maas, 1994; Wall and Hogan, 1995; Wu et al., 2004; Zirzowa et al.,

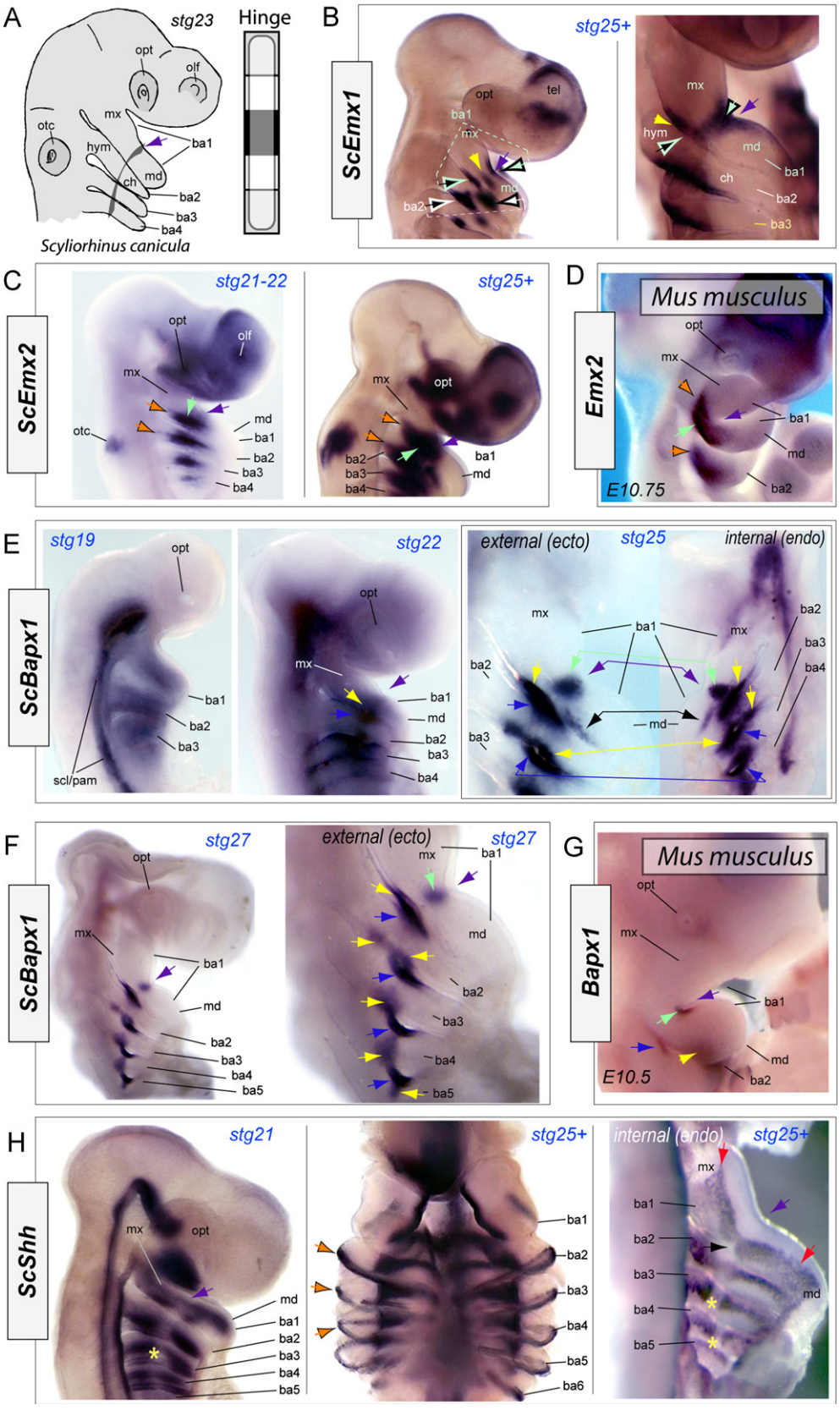

2009); (2) a gene, *Hand2*, solely associated in amniotes (and osteichthyans) with the distal midline of mdBA1 and the more caudal BA (Thomas et al., 1998; Kuraku et al., 2010; Miller et al., 2003; Fig. 7); and (3) a gene, *Raldh3*, solely associated in amniotes with the proximal BA1 associated with the λ-junction (Dupe et al., 2003; Compagnucci et al., 2011) (Fig. 7).

Genes expressed in amniotes in both sets of 'Caps' can be further sub-categorized in a number of ways, including through separation of those differentially expressed in epithelial cells of one cap and mesenchymal cells in the other (such as *Dlx3*) and those expressed the same type of cells in each cap, such as *Prx1* in the mesenchyme. With regard to the former, and as described above, *ScDlx3* is indeed expressed in the mesenchyme of BA1 of the shark distal to the MMC while in the epithelium of the proximal mxBA1 (Fig. 6B and C). It is further expressed in the epithelium associated with the olfactory placode but is not expressed in epithelial cells bridging the placode with mxBA1.

Prx1, moreover, bears a notable level of conservation between its expression in amniotes and chondrichthyans (compare Fig. 6D and E). Both Sc*Prx1* and *Prx1* are expressed in the polar ends, or caps, of BA1 (blue and white arrows at the mxBA1 portion of the λ-junction and blue arrows at the distal end of mdBA1) in their respective taxonomic correlatives. Each, moreover, displays a distinct oral/rostral-aboral/caudal separation in expression (compare blue and yellow arrows with blue and white arrows in Fig. 6D, stage 23 and 6E), especially within the proximal BA, including a distinguished caudal swath of expression in cells of the proximal BA2 (green arrows, Fig. 6D and E). This oral/aboral separation correlates with the discrete bulges in the BA1 identified in the scanning electron micrographs (Fig. 3E). Notably, at early stages of BA development, *ScPrx1* expression is expansive throughout the caudal BA but with ontogenetic progression expression becomes restricted to the caps. In the mouse, the mxBA1 and mdBA1 domains are connected by a small bridge of expression, which is absent in the shark.

As with *Msx1* in amniotes, *ScMsx1* transcripts are found in the mesenchyme of both proximal and distal caps in pharyngula stage shark embryos (Fig. 6F and G). Similar to *ScPrx1*, *ScMsx1* is initially expressed extensively through the BA as they form (stage 22, Fig. 6F) but becomes restricted to the caps regions with ontogenetic progression of each BA (stage 25+, Fig. 6F). Notably, the oral/aboral polarity evinced with *ScPrx1* in the proximal BA is also encountered with *ScMsx1* (see blue and white and blue and yellow arrows, Fig. 6F), though in the caudal BA transcripts appear aborally restricted. There are, however, differences with murine expression evident: for instance, while *Msx1* is continuously expressed from the frontonasal processes through the mxBA1 at the λ-junction, *ScMsx1* is not. Moreover, a thin hinge-positioned proximo-distal line of *ScMsx1* expression is seen in BA1 of *S. canicula*, although whether this has any correlation with the symmetrical expression of amniote *Msx1* at the hinge region is unclear (green arrows, Fig. 6F and G). Furthermore, *ScTbx2* expression, which is rather dynamic, bears a numbers of similarities with *ScMsx1* and *ScPrx1* and is likewise caps-centric in expression (Fig. 6H and I).

Bmp4 expression in the caps epithelium of the amniote BA1 of both the λ-junction and distal mdBA1 midline (Fig. 6K) has been well recorded (e.g., Abzhanov et al., 2004; Ashique et al., 2002; Barlow and Francis-West, 1997; Bei and Mass, 1998; Foppiano et al., 2007; Gong and Guo, 2003; Lee et al., 2001; Liu et al., 2005a, 2005b; Shigetani et al., 2000) and was a distinct component of the evidential scaffold establishing the 'Hinge and Caps' model (see Depew and Simpson, 2006). In *S. canicula* embryos, *ScBmp4* transcripts are detectable in the distal mdBA1 (blue arrows, Fig. 6J) and the proximal, maxillary BA1 (blue and white arrows, Fig. 6J). Although *ScBmp4* is expressed in the optic primordia, just as *Bmp4* is in the mouse, we failed to detect frontonasal expression connecting with mxBA1 in shark embryos.

The osteichthyan BA, including those of the mouse, are characterized by *Hand2* expression solely at their distal, or mandibular cap, ends (light green arrow, Fig. 7C). This pattern is ancestral for gnathostomes as it likewise characterizes the BA of *S. canicula* embryos (light green arrows, Fig. 7B). The opposite, or λ-junctional, pole of amniote BA1 in early pharyngula stage embryos, moreover, is characterized by the expression of *Raldh3* (Fig. 7F; Dupe et al., 2003), a gene encoding a dehydrogenase involved in the synthesis of the potent signaling molecule, retinoic acid (Brickell and Thorogood, 1997). Indeed, in murine embryos at E9.5, *Raldh3* transcripts are typically found in the optic primordia and ventrally in the ectoderm positionally located between the proximal most mxBA1 and the edge of the olfactory placode, while by E10.5 transcripts are more restricted, being detected in the optic primordia and the ventral olfactory pits (i.e., associated with the λ-junction) (Fig. 7F). In a manner akin to E9.5 murine embryos, stage 21 *S. canicula* embryos express *ScRaldh3* in the optic primordia as well in the ectoderm between the proximal-most mxBA1 and the edge of the olfactory placode (Fig. 7E). In line with homologous expression in the E10.5 murine embryo (Fig. 7F), *ScRaldh3* continues to be expressed in the optic primordia of stage 25+ shark embryos, as well as in cells associated with the ventral most portion of the olfactory pit (Fig. 7E); in the shark embryo, however, additional circum-optic expression is encountered at this later stage.

Detection of heterotopic patterns of gene expression between amniote and Scyliorhinus canicula embryos: Exemplars

While we were interested in assessing whether a basic 'cap-to-hinge-to-cap' architecture of gene expression was a shared feature of gnathostome craniofacial primordia, we were equally interested in discerning the possible presence of heterotopic and/or heterochronic patterns in gene expression between amniote and chondrichthyan embryos. Below, we present three further examples of heterotopic patterns of gene expression of varying degrees between amniotes and chondrichthyan embryos.

As the *Alx* homeobox genes are thought to have disparate patterns of gene expression in tetrapods (McGonnell et al., 2011), we examined the expression of one member of this family, *Alx4*, in pharyngula stage *S. canicula* embryos. In amniotes, *Alx4* is

Fig. 5. Hinge-centric gene expression in *S. canicula*. (A) Schema delineating the expected positioning of hinge-centric patterns of gene expression. The purple arrow indicates the maxillary–mandibular constriction (MMC). (B) *ScEmx1* at stage 25+. Black-bordered green arrow indicates oral expression at the mmc, while the connected green-bordered black arrow indicates aboral ba1 expression. The yellow arrow highlights lateral, centralized ba1 expression. The connected black and white arrows indicate the disto-rostral and proximo-caudal offset of expression, aligned at the hinge region, characteristic of ba2 and the more caudal BA. ((C), (D)) Comparative shark (C) and murine (D) *Emx2* expression patterns. Light green arrows emphasize the conserved nature of hinge-centric expression. The black-bordered orange arrows emphasize a proximal extension of expression. Purple arrows indicate the maxillary–mandibular constriction. ((E)–(G)) Comparative shark ((E), (F)) and murine (G) *Bapx1* expression patterns. The purple arrows pinpoint the MMC, while the light green arrows indicate MMC-centered expression. The yellow and blue arrows highlight the dynamic juxtaposition of caudal (yellow) and rostral (blue) BA expression centered at the pharyngeal clefts. (H) *ScShh* expression emphasizes the notion that hinge-centric expression includes relative absence of expression (yellow asterisks, black arrow) as well as relative abundance. Red arrows indicate the oral limit to the pharyngeal endodermal expression. Purple arrows indicate the MMC. The black-bordered orange arrows emphasize the distinctive proximo-distal ectodermal lines of expression in the BAs. *Abbreviations*: ba1–6, branchial arches 1 through 6; ch, ceratohyal branch of the second branchial arch; hym, hyomandibular second branchial arch; md, mandibular first branchial arch; mx, maxillary first branchial arch; olf, olfactory primordia; opt, optic primordia; otc, otic primordia; scl/pam, scleratomal paraxial mesoderm; stg, stage.

expressed in a caps pattern, being detected in the both the mxBA1 and FNP of the λ-junction and in the distal midline of mdBA1 (McGonnell et al., 2011; Twigg et al., 2009, and Supplementary Fig. 3B). Moreover, in chicks – but not in mice – *Alx4* is also expressed circum-orbitally. *ScAlx4* is detected circumscribing the developing eye, as well as in the developing FNP, like its

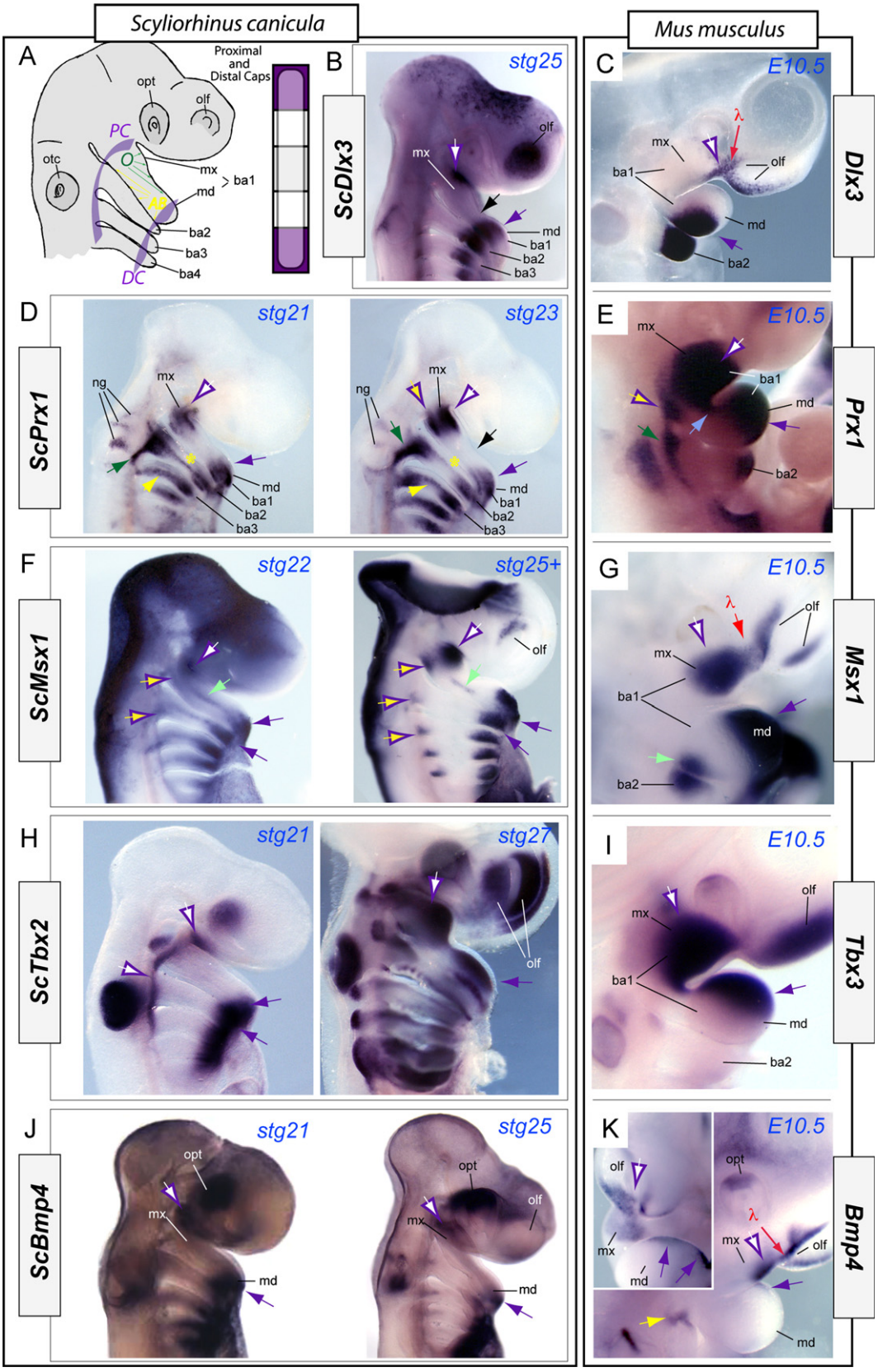

orthologue in the chick (Supplementary Fig. 3A). However, we failed to detect significant *ScAlx4* signal in mdBA1 mesenchyme in stage 21 to 27 shark embryos.

Meis genes encode proteins that form dimerization partners with the protein products of *Pbx1-3*, genes that have recently been implicated in playing significant-tissue specific roles in amniote craniofacial development (Ferretti et al., 2011; Selleri et al., 2001), as well as acting as Hox-cofactors. We therefore examined *ScMeis2* expression in *S. canicula* embryos (Supplementary Fig. 3C). We found that, as might be expected of a *Hox* co-factor, *ScMeis2* expression is absent in BA1 in stage 20 and 23 *S. canicula* embryos although significant proximo-distal lines of expression were detected from BA2 and the caudal BA. Unlike what we see with its murine orthologue (Supplementary Fig. 3D), significant levels of *ScMeis2* were also found associated with the optic primordia (black arrows, Supplementary Fig. 3C). In line with amniote expression, *ScMeis2* was detected in the FNP and in mxBA1 (yellow arrow, Supplementary Fig. 3C) though, unlike in amniotes, it was not detected in the non-optic cells between the two. In contrast to what we found with *ScMeis2*, murine *Meis2* is also found in mdBA1 and in a more significant proportion of BA2.

Fgf8, encoding a fibroblast growth factor with significant developmental roles during development, has distinct cephalic expression patterns during ontogeny (Fig. 8; Abu-Issa et al., 2002; Abzhanov and Tabin, (2004); Compagnucci et al., 2011; Crossley and Martin, 1995; Neubüser et al., 1997; Song et al., 2004; Szabo-Rogers et al., 2008; Trumpp et al., 1999; Tucker et al., 1999). In both the chick and mouse, for instance, *Fgf8* is expressed in the isthmus (the midbrain/hindbrain boundary), in the ventro-lateral cephalic ectoderm (including the lining of the olfactory pits), in the pharyngeal plates, and, significantly, in the hinge-centric oral ectoderm of both mxBA1 and mdBA1 (Fig. 8D and E). One notable distinction between the chick and the mouse, however, is that in the mammal *Fgf8* expression along the dorsal olfactory pit spreads ventrally during ontogeny and eventually unites at the λ junction with the ectoderm of the mxBA1 (see red arrows, E10.5 embryo, in Fig. 8E) while that in the avian does not (as exemplified by red arrows in the HH23 embryo, Fig. 8D). As with the amniote embryos, *ScFgf8* is detected at the isthmus and in the ventro-lateral cephalic ectoderm, including in the dorsal olfactory pit (Fig. 8B and C). *ScFgf8* is also significantly expressed in both the rostral/oral and caudal/aboral aspects of the pharyngeal clefts. Strikingly at odds with what is seen with the amniotes, however, we failed to detect expression within the oral ectoderm of either mxBA1 or mdBA1 of the shark embryo.

Discussion

As their taxonomic appellation implies, jaws have been of central importance to the evolution and diversification of gnathostomes. Tracing the paleontologic pattern of the intricate evolution of jaws and their associated structures has long been an active endeavor. More recently, approaching a molecular, cellular, and genetic reconstruction of this pattern has also come to the fore to partner these studies.

The seminal evolutionary event leading to jaws appears to have been the acquisition in an ancient agnathan taxa – possibly one related to a diplorhinic ostracoderm – of a segmented, articulated, iterated branchial skeleton (Fig. 1; Forey and Janvier, 1993; Gai et al., 2011; Gregory, 1933; Janvier, 1993, 1996; Kuratani, 2012; Kuratani et al., 2012; Mallatt, 1997; Moore, 1981; Radinsky, 1987; Romer, 1966; Young, 1981). From this, the first gnathostome fish subsequently appeared, over 400+ million years ago, and rather quickly thereafter four major groups of jawed fish appeared: Placoderms, Acanthodians, Chondrichthyans and Osteichthyans (Carroll, 1988; Janvier, 1996; Jarvik, 1980; Jollie, 1962; Moy-Thomas and Miles, 1971; Miles, 1964; Schultze, 1993; Watson, 1937). In line with a fundamental reorganization of the agnathan crania, these first gnathostome fish all possessed paired nostrils, paired nasal capsules and paired trabecula cranii, as well as three semicircular canals: notably, moreover, these initial gnathostomes shared a fundamental design and structural organization to their jaws, features that have been conserved attributes of all subsequent gnathostomes (e.g., Barghusen and Hopson; 1979; de Beer, 1985; Goodrich, 1958; Gregory, 1933; Halstead, 1968; Hildebrand, 1988; Moore, 1981; Schultze, 1993). Placoderms, however, possessed a number of anatomical features differing from the other three groups: for instance, the placodermal PQ was lateral to the jaw musculature rather than being medial and typically a joint formed between the well sutured (but rigid) head and the shoulder portions (Carroll, 1988; Dean, 1909; Maisey, 2001; Schaeffer and Williams, 1977). Such differences, among others, have suggested to many that Placoderms were derived from a basal lineage different than that giving rise to the Acanthodians and the extant gnathostomes (Davis et al., 2012; Schaeffer and Williams, 1977).

The evolutionary inter-relationships between the other three groups – the Acanthodians, Chondrichthyans, and Osteichthyans – have been somewhat more elusive but have been intriguing points of investigation for some time (Brazeau and Ahlberg, 2006; Carroll, 1988; Davis et al., 2012; Dean, 1909; Halstead, 1968; Holmgren, 1942; Miles, 1964; Schaeffer and Williams, 1977; Schultze, 1993; Watson, 1937). Acanthodians, though restricted to the Paleozoic, are particularly significant in these investigations as they constitute one of the oldest known groups (if not the oldest) of gnathostomes and possessed characteristics of both Chondrichthyans and Osteichthyans. For instance, they possessed bony cranial skeletal elements but also had upper jaw PQ elements with shark-like morphology (Carroll, 1988). Historically, the questions have been whether Acanthodians were thus to be aligned with basal sharks or with basal bony fish and what this then might tell us about which morphologic (or, by extension with the extant groups, what molecular) character states might be ancestral (plesiomorphic) and which derived (apomorphic) in nature.

Fig. 6. Comparative shark (*S. canicula*) and murine (*Mus musculus*) caps-centric gene expression. (A) Schema delineating the expected positioning of caps-centric patterns of gene expression. PC: proximal cap. DC: distal, mandibular cap. O: oral. AB: aboral. ((B), (C)) Comparison of shark *ScDlx3* (B) and mouse *Dlx3* (C) expression evincing a distinct conservation both of the mesenchymal expression (purple arrows) distal to the maxillary–mandibular constriction (MMC; black arrows) and of the maxillary and olfactory ectoderm (purple-bordered white arrows). Unlike the shark, the mouse has continuous expression of *Dlx3* at the lambdoidal junction (λ). ((D), (E)) Comparative *Prx1* expression. Purple-bordered white arrows indicate rostro-proximal caps expression associated with the maxillary ba1 while purple arrows point to distal caps expression. Purple-bordered yellow arrows indicate distinct caudo-proximal maxillary expression. The dark green arrows highlight the distinct trans-ba2 swath of expression of *Prx1* evinced in the proximal-most ba2 of both the shark and the mouse. Black arrow: mmc. The yellow arrows and asterisks in the stage 21 and stage 23 shark embryos highlight the notion that a proximo-distally oriented medial line of transcript is initially found in the post-ba1 arches but which dissipates during ontogeny. ((F), (G)) Comparative *Msx1* expression. Arrows as above though the purple-bordered yellow arrows indicate the proximo-caudal aspect of the caudal BA in addition to that of ba1. The light green arrows indicate hinge-centered expression that appears as a proximo-distally oriented medial line in the shark and at the first pharyngeal plate in the mouse. The red arrow in the mouse highlights the continuity of expression at the lambdoidal junction (λ) of the mouse. ((H), (I)) *S. canicula* (H) and *M. musculus* (I) expression of *Tbx* genes. Arrows as above. ((J), (K)) Comparison of *ScBmp4* and *Bmp4* expression. Yellow arrow indicates expression in ba1 and ba2 at the first pharyngeal cleft in the mouse. Other arrows as above. *Abbreviations*: ba1–6, branchial arches, 1 through 6; hym, hyomandibular second branchial arch; md, mandibular first branchial arch; mx, maxillary first branchial arch; ng, neuroganglia; olf, olfactory primordia; opt, optic primordia; otc, otic primordia; stg, stage; λ, lambdoidal junction.

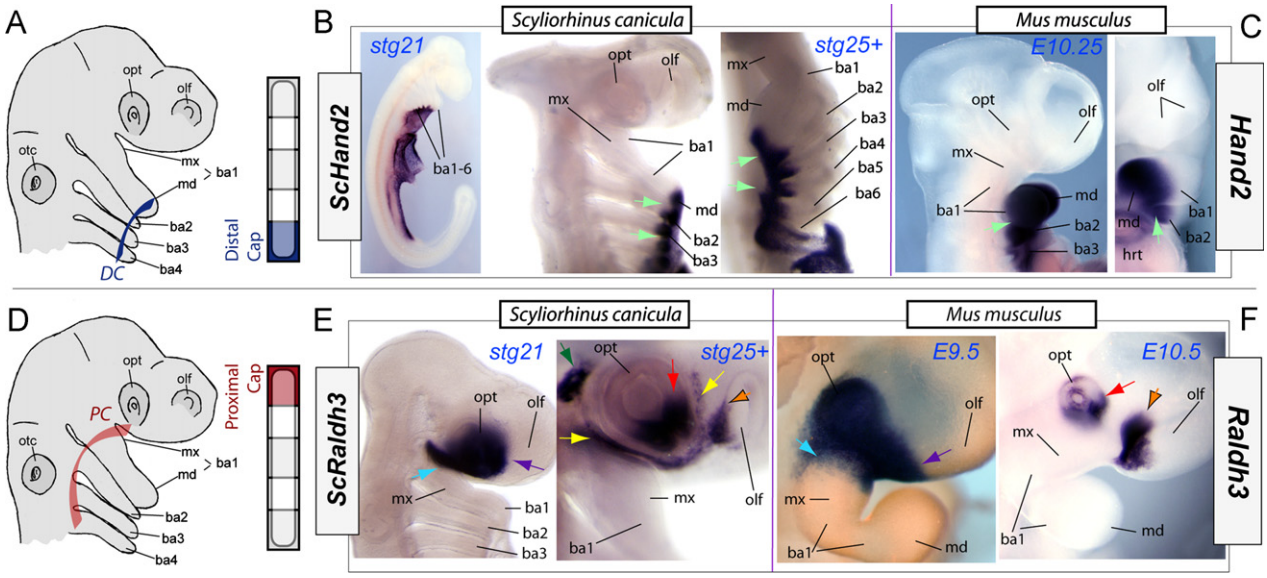

Fig. 7. Conserved expression of restricted proximal caps and restricted distal caps expression in shark (*S. canicula*) and murine (*M. musculus*) embryos. (A) Schema delineating the expected positioning of restricted distal-cap pattern of gene expression. DC: distal, mandibular cap. ((B), (C)) Comparison of *Hand2* expression in shark (B) and mouse (C). Green arrows highlight the pattern of expression restricted to the distal BA. (D) Schema delineating the expected positioning of restricted proximal-cap pattern of gene expression. PC: proximal, maxillary cap. ((E), (F)) Comparison of *Raldh3* expression in shark (E) and mouse (F). The light blue arrows in the stage 21 *S. canicula* and E9.5 *M. musculus* embryos indicate early expression in the maxillary ba1 near the optic primordia, while the purple arrows indicate the rostro-ventral extent of expression in the cephalic ectoderm subjacent to the optic primordia and caudal to the olfactory primordia. The red arrows point to the expression in the ventral optic primordia and the black-bordered orange arrows indicate olfactory expression. The yellow arrows on the later stage shark embryo highlight cephalic ectodermal expression between the ventral optic apparatus and the olfactory and maxillary cells. *Abbreviations*: ba1–6, branchial arches, 1 through 6; hym, hyomandibular second branchial arch; md, mandibular first branchial arch; mx, maxillary first branchial arch; olf, olfactory primordia; opt, optic primordia; otc, otic primordia; stg, stage; λ, lambdoidal junction.

Recent investigations, including principle component (phenetic) analysis coupled with phylogenetic analysis of Acanthodian, Chondrichthyan and Osteichthyan crania, have suggested that the more shark-like characteristics of Acanthodians are, in fact, shared ancestral states (symplesiomorphic) for crown group gnathostomes: that is, the last common ancestor of extant gnathostomes was *shark*-like (rather than bony fish-like) in morphologic specificity and character (Davis et al., 2012; Brazeau, 2009). Thus, our advances in the understanding of the molecular, cellular and genetic characteristics of the developing shark jaw primordia yield further insight into the basal organizational state of the gnathostome jaw and subsequently provide a platform for investigations into the patterning mechanisms underlying jaw development and evolution throughout the Gnathostomata.

Pattern and polarity in gnathostome jaw development

Herein, we have presented an anatomical and molecular examination of early jaw development, conceptually centered around the 'Hinge and Caps' model, in embryos of the lesser spotted dogfish shark, *S. canicula*. One patent purpose was to gain insight into the basal molecular organizational state of the gnathostome jaw primordia, as epitomized by this particular elasmobranch, and then initiate a comparison with other gnathostome taxa by searching for evidence of heterotopic and/or heterochronic patterns of gene expression through comparison with other taxa about which we have a greater degree of understanding of their jaw development—namely the amniotes *Gallus gallus* (chicks) and *Mus musculus* (mice).

Though a developmental staging series (followed herein) has been put forth for early *S. canicula* embryos (Ballard et al., 1993) it does not give any specific thought to the relative development of the craniofacial primordia that give rise to the jaws. To facilitate subsequent comparisons with amniote development, we followed this staging series and utilized scanning electron microscopy to examine the ontogeny of the early embryonic development of *S. canicula*, paying particular attention to the relative development of the BA and the olfactory, optic, otic, and hypophyseal placodes and pits (Fig. 3). From our SEM analysis, it became clear that proximo-distal, medio-lateral and rostro-caudal polarities in morphology are patent early in shark BA ontogeny and that some of these polarities are iterative within the BA as a series. Thus both the jaws and their primordia exhibit polarity; a significant consequence of such developmental polarity is the potential for the establishment of modularity in jaw construction (Depew and Compagnucci, 2008; Fish et al., 2011).

We found that polarity of gene expression patterns also characterizes the developing branchial arches of *S. canicula*. For instance, along the proximo-distal axes of the BA, we recognized at least four basic patterns: (1) expression centered at the midpoints of the BA (i.e., at the 'hinge'), as evinced by *ScBapx1*, *ScEmx1*, and *ScEmx2*; (2) expression, complementary to this first category, at the polar ends of the BA (i.e., the 'caps'), as exemplified by *ScMsx1*, *ScPrx1*, *ScTbx2*, and *ScBmp4*; (3) nested expression of related genes, such as the tiered, terraced nesting of *ScDlx1/2*, *ScDlx3/4* and *ScDlx5/6*; and (4) expression confined to one BA1 polar extreme or the other, as typified by expression of *ScHand2* in the distal-most mdBA1 and *ScRaldh2* at the proximal end of mxBA1. These patterns also characterize the amniote state.

Sharks and modeling the etiology of BA polarity and modularity in jaw development

Because modularity plausibly explains both integration within jaw structures and autonomy between jaw structures, as well as potentially providing a mechanism for evolutionary modifications and transformations of jaws, understanding the developmental origins of polarity and modularity within the developing jaws is a key endeavor in addressing jaw development and evolution (Fish et al., 2011). Current models of jaw development typically

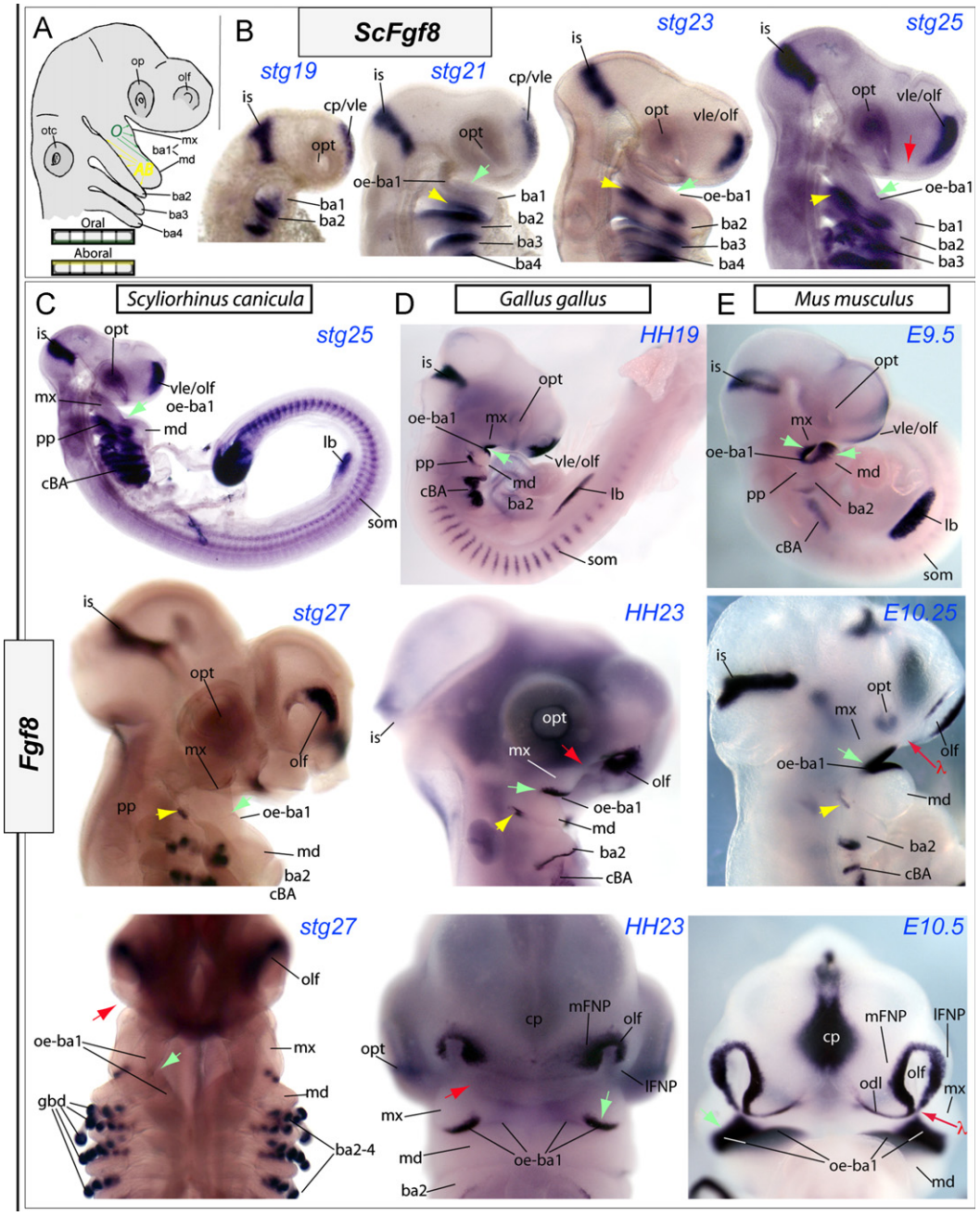

Fig. 8. Notable heterotopy of *Fgf8* expression in the oral ectoderm. (A) Schema delineating the expected positioning of caps-centric patterns of gene expression. O: oral (in green). AB: aboral (in yellow). ((B), (C)) *ScFgf8* in *S. canicula* embryos ranging from stage 19 to stage 27. Green arrows indicate the oral ectoderm, while yellow arrows indicate the pharyngeal clefts formed from the plates. Red arrows highlight the ectoderm between the olfactory pit and mxBA1. (D) *Fgf8* in HH19 and HH23 chick (*G. gallus*) embryos. Red arrows highlight the positioning of the λ junction, while other arrows are as above. (E) *Fgf8* in E9.5, E10.25 and E10.5 mouse (*M. musculus*) embryos. Arrows are as in '(D)'. *Abbreviations*: ba1–6, branchial arches, 1 through 6; cBA, caudal branchial arches; cp, commissural plate; gbd, gill bud; is, isthmus at midbrain-hindbrain boundary; lb, limb bud; lFNP, lateral frontonasal process; md, mandibular first branchial arch; mFNP, medial frontonasal process; mx, maxillary first branchial arch; odl, odontogenic line; oe, oral ectoderm; olf, olfactory primordia; opt, optic primordia; otc, otic primordia; pp, pharyngeal plate; som, somite; stg, stage; vle, ventro-lateral cephalic ectoderm; λ, lambdoidal junction.

address, at a minimum, the polarity of BA gene expression patterns and subsequent structure in the developing jaws.

For example, genetic and experimental manipulation mainly in zebrafish and lamprey embryos, but including some murine studies, coupled with analysis of basic patterns of gene expression, has led to one model of 'dorso-ventral' polarity of the BA that postulates the presence of a regulatory network involving the 'ventral' (i.e., topographically synonymous with 'distal' as used herein) expression of *Bmp4* and *Endothelin 1* (*Edn1*), and their *Msx* and *Hand2* targets, reciprocally regulating (in part through *Mef2c*) the nested *Dlx* genes to establish a combinatorial expression code which resolves into zones within the developing BA of 'ventral' and 'intermediate' nature (e.g., Talbot et al., 2010; Medeiros and Crump, 2012; Tavares et al., 2012). In this model, the intermediate zone becomes permissive of 'jaw joint' formation as revealed by the eventual induction of *Bapx1* (*Nkx3.2*), and a 'dorsal' (proximal) zone is further established by repulsion of the intermediate zone. At the heart of this mandibular-centric model, however, is the establishment of the ventral/distal zone as established by Edn1 signaling as dorso-ventral polarity is posited to flow form this.

We find that a number of patterns of gene expression in *S. canicula* are, on their surfaces at least, in line with such a model. *ScHand2*, as a presumed target of Edn1 signaling in the shark, is distally (ventrally) expressed in the BAs. Likewise, both *ScBmp4* and its presumptive target, *ScMsx1*, are expressed in the distal BAs. We further find that *ScDlx* genes are nested, and that *ScBapx1* is expressed around the MMC, which is in line with a potential intermediate position.

A number of additional, compounding factors, however, must be taken into consideration when modeling the etiology of polarity and modularity within the developing jaws: For instance, in addition to establishing a developmental mechanism to regulate and elaborate the inherent polarity of the BA, it is patent that whatever patterning mechanisms inform the developing jaw primordia must (1) account for the functional integration and registration of the upper jaws with the lower jaws (and neurocranium) as well as (2) be tractable to potential selective pressures for disparate upper and lower jaw development (Depew and Compagnuicci, 2008; Depew and Simpson, 2006; Fish et al., 2011).

These additional notions are fundamental to, and explicit within, the 'Hinge and Caps' model, making this model distinct from other models (such as the one described above) of jaw polarity and modularity. This particular model posits that the achievement of notions 1 and 2 above is possible if the patterned placement of the articulation of the upper and lower jaws – the position where registration is absolutely required – is balanced by patterned placement of the developing tips of both the upper and lower jaws, i.e., the proximal-most mxBA1 and distal-most mdBA1. Jaw registration is thus plausibly achieved by the integration of patterning cues from the hinge-associated region with those from each of the two caps. In effect, epithelial-mesenchymal interactions emanating from the *hinge* region, integrating with those from the *caps*, set up coordinated, polarized BA tissues: Polarity is thus oriented *from* hinge *to* cap for both the developing upper and the lower jaws (see arrow orientation in Fig. 2c and d). Integrated signaling along the polar axes subsequently partitions the developing jaw primordia into multiple nested and overlapping developmental fields (discussed in Fish et al., 2011). Within these developmental fields of the jaw primordia, relatively independent sets of character states, including focalized autonomous cellular behaviors, are encountered. One reflection of such behaviors is the presence of coordinated cellular transcription within subpopulations of each primordia: Understanding that modules can be minimally defined as units consisting of integrated characters that are relatively independent of other characters, these focalized autonomous cellular behaviors delineate modules.

The 'Hinge and Caps' model suggests at least two significant, testable notions with regard to polarity and modularity in the BA. First, it would be expected that a hallmark of hinge-associated patterning cues would be the expression of genes in a symmetrical pattern within the center of the proximo-distal axis of BA1 (i.e., at the mxBA1–mdBA1 junction, or MMC) and caps-associated patterning cues by the balanced expression of genes likewise symmetrically expressed at *both* caps. These expectations are indeed met with in *S. canicula* embryos. As noted above, analysis of *ScBapx1*, *ScEmx1* and *ScEmx2* expression demonstrated that these genes are expressed in the center of the proximo-distal axes of the BA (e.g., at the MMC) and represent conserved, hinge-associated genes in gnathostomes. Moreover, we found evidence of balanced expression of genes symmetrically expressed at *both* caps of the BA, as exemplified by *ScMsx1*, *ScPrx1*, *ScTbx2*, and *ScBmp4*. This pattern of hinge-to-both caps expression is notably associated with the bi-directional pattern of gill bud florescence emanating from the BA-midpoints to the caps ends.

Second, the 'Hinge and Caps' model posits a correlation between patterns of expression and modular behavior during development. Gnathostome BAs are meristic (segmentally repeated) vertebrate structures. One demonstration of modularity in development of meristic structures is their capacity for homeotic transformation. Homeosis has been demonstrated for the BA of amniotes, which are metameric both between each other within the rostro-caudal series and within each individual arch along the proximo-distal axis (e.g., Beverdam et al., 2002; Depew et al., 2002a,b; Goodrich, 1958; Halstead, 1968; Kuratani, 2004, 2005, 2012; Nelsen, 1953; Rijli et al., 1993). Developmental mechanisms are in place to ensure that each BA of the series acquires a unique identity and that each structure within the proximo-distal axis of each arch does so as well. It is believed that regional specification of metameric structures is controlled by the nested expression of related genes resulting in a regional code: such is the case with the amniote BA, where the *Hox* and *Dlx* gene families regulate inter- and intra-BA identity, respectively (reviewed in Depew et al., 2005; Kuratani, 2004, 2012; Minoux and Rijli, 2010).

Individual BA-identity as regulated by the rostro-caudally nested *Hox* genes has been well investigated in mice. The genetic ablation in mice of *Hoxa2*, whose proximal-most BA expression is BA2, yields skulls with a notable enantiomorphic homeotic transformation of BA2 jaw-related structures into BA1 structures (Rijli et al., 1993). Significantly with regard to the polarity of the developing jaws, it is those structures formed nearest to the hinge region – a region topographically akin to the MMC in the shark embryo – associated with the pharyngeal plate between BA2 and BA1 that are found to be transformed in these mice. Together, with anatomical and paleontological evidence demonstrating that basal gnathostomes exhibit significant reliance on the coordination of BA2 skeletal structures with BA1 structures for the important task of connecting their jaws to their neurocrania (Barghusen and Hopson, 1979; de Beer, 1985; Carroll, 1988; Gregory, 1933; Halstead, 1968; Jollie, 1962; Maisey, 2001, 2008; Romer, 1966; Schaeffer and Williams, 1977; Wilga, 2002), this suggested the presence of a focal BA-associated source of patterning information centered at the hinge region—a notion that is very much in line with the 'Hinge and Caps' model.

Hox profiles have recently been examined in chondrichthyans, including in *S. canicula* and the holocephalan *Callorhincchus milli* (Freitas et al., 2006, 2007; Mulley et al., 2009; Oulion et al., 2011; Ravi et al., 2009; Rodriguez-Moldes et al., 2011; Sakamoto et al., 2009). Studies of *ScHoxa2* indicate that a rostral expression limit set at BA2 is ancestral for *Hoxa2* orthologues. Likewise, expression profiling of *ScOtx2*, thought to be a default marker of BA1 as it is expressed throughout BA1 but not in the caudal BA (Kuratani, 2005; Matsuo et al., 1995), has suggested amniote *Otx2* likewise represents a conserved cognate (Germot et al., 2001; Plouhinec et al., 2005). Thus, it appears that this core molecular architecture for inter-BA identity is a conserved feature of gnathostomes. It is worth noting, however, that we did find differences in BA expression profiles of genes implicated as co-factors for the *Hox* genes, including between the TALE co-factor *ScMeis2*/*Meis2* orthologues (Fig. 8C).

To correlate intra-BA morphologic polarity and potential modularity in *S. canicula* with its plausible genetic etiology, we asked whether *S. canicula* embryos displayed an amniote-like nested pattern of *Dlx* expression in their developing BA. We found that *S. canicula* embryos did indeed display an overall amniote-like pattern of tiered, terraced nesting of *Dlx* genes (Fig. 4 and Supplementary Figs. 1 and 2), which makes such nesting of *Dlx* genes ancestral (symplesiomorphic) for crown group gnathostomes. Moreover, although it has been suggested that *Dlx2* orthologues may be expressed in CNC only once they enter the BA (see Blentic et al., 2008), we detected the presence of *ScDlx2*

transcripts in streams of CNC entering the shark BA just as has been seen with mice (Fig. 4F). A number of differences in cephalic *Dlx* expression between the shark and chicks and mice are, however, notable. For instance, a regression, similar to that seen by stage 27 in *ScDlx2* expression, from the mdBA1 to a position proximal to the MMC has yet to be reported for any other *Dlx2* orthologue in a similarly staged amniote embryo. This regression is accompanied by an expansion of *ScDlx5* expression proximal to the MMC in later stage embryos. It is uncertain whether such an expansion in *ScDlx5* represents either a heterotopy or heterochrony as a similar expansion actually occurs in murine embryos after E10.5 and in chick embryos at later stages; what is distinct in *S. canicula* expression, however, is the oral–aboral asymmetry in expression in this proximal *ScDlx5* domain.

Notably, extant agnathans such as the lamprey have a BA skeletal architecture that is neither hinged nor articulated and thus they do not have jaws: this lack of articulated segmentation within the BA is correlated with a pattern of *Dlx* gene expression that is not nested (Kuraku et al., 2010; Kuratani, 2005, 2012; Neidert et al., 2001; Myojin et al., 2001; but also see Cerny et al., 2010). A number of issues regarding the relationship between *Dlx* nesting and jaw evolution are outstanding, however: It remains unclear, for instance, whether *Dlx* nesting is a prerequisite for articulated segmentation, and therefore for jaw formation, or if it is simply a permissive factor (though the latter might seem most parsimonious). Approaching these questions is now possible as a much more comprehensive comparative analysis of vertebrate *Dlx* gene expression and biology is now a salient, achievable goal.

The developmental mechanism patterning the gnathostome BA thus includes a molecular baüplan involving the coordinated, nested expression of *Hox* (plus *Otx*) and *Dlx* genes. Such nesting reflects the potential for modularity, and evidence from the expression of *ScHox* and *ScDlx* genes in *S. canicula* embryos therefore supports a correlation between patterns of expression and modular behavior in gnathostome BA development.

The evolving upper jaw: On the maxillary BA1 and eventual FNP involvement in gnathostomes

Although a coordinated *Hox-Dlx* grid might regulate both inter- and intra-BA skeletal identity, it is clear that proximo-distal polarity in BA1 involves more than just nested *Dlx* gene expression (Depew and Compagnuicci, 2008; Depew and Simpson, 2006). Indeed, even the lack of an articulated BA skeleton does not mean that a proximo-distal polarity is absent in the BA of the jawless lamprey: For instance, an inherent molecular polarity is attested to by the distally restricted expression of the *Hand2* orthologue in the developing lamprey BA (Cerny et al., 2010; Kuraku et al., 2010; Kuratani, 2012). Such distal restriction appears to be a shared character state of the vertebrate BA as all known gnathostome *Hand2* orthologues (Fig. 7) are distally restricted in the BA, though this does not mean that the extent and nature of such restriction is conserved (for instance, see arguments presented Kuratani, 2012). *ScHand2* and *Hand2* epitomize gene orthologues restricted to the mdBA1 'Cap': This restriction is not unexpected when consideration is given to the fact that during their ontogeny the BA are topographically positioned between the developing heart and the brain. The distal domains of the BA develop in close association with the heart, and it is thus perhaps of little surprise that integrative patterning involving cognate genes such as *ScHand2* and *Hand2* is a feature of regional development of both the heart and the distal BA. Indeed, functional studies demonstrate that *Hand2* regulates both cardiac and jaw development (Yanagisawa et al., 2000).

Likewise, it is not unexpected that genes, such as *ScRaldh3–Raldh3* (Fig. 7), exist that characterize the developing nervous system and the juxtaposed proximal-most mxBA1 'Cap' but not the mdBA1 'Cap'—especially when considering that the upper jaws are more intimately associated with the neurocranium than are the lower jaws. Such genes highlight the facts that 'maxillary BA1' is more than just 'non-mandibular BA1' and that formation of the upper jaws is more than just an afterthought to the formation of the lower jaws and trabeculae cranii (i.e., rostral neurocranium). Indeed, mdBA1 expression of 'Caps' related genes is equally represented by mxBA1 'Caps' expression: In the expression patterns of *ScMsx1*, *ScPrx1*, and *ScTbx2* we note an overall correspondence between the amniote and chondrichthyan homologues with regards to dual (presumably coordinated) 'Caps' expression (Fig. 6).

Notably, amniote *Bmp4* expression in the 'Caps' epithelium of both the λ-junction and distal mdBA1 midline and in the pharyngeal plate region (as well as functional data stemming from gene-targeting experiments in mice) provided substantive evidential support to the 'Hinge and Caps' model (see Depew and Simpson, 2006; Depew and Compagnuicci, 2008); *ScBmp4* transcripts are similarly detectable in the distal mdBA1 as well as in the proximal mxBA1. Two areas of difference in expression are notable, however. First, we did not detect an *ScBmp4* pharyngeal plate expression pattern topographically akin to that of amniote *Bmp4* (Fig. 6). Second, though *ScBmp4* is expressed in the optic primordia, just as its orthologue *Bmp4* is in the mouse, frontonasal expression connecting with mxBA1 is absent in shark embryos. Such a lack of connection, or continuity of expression, between the developing fronto-nasal/olfactory apparatus and mxBA1 is a common theme with the gene expression patterns of chondrichthyans, also characterizing, for example, *ScDlx2*, *ScDlx3*, *ScMsx1* and *ScMeis2* expression.

This lack of expression highlights a central difference between elasmobranch chondrichthyans and osteichthyans in the elaboration of the developing upper jaw's association with the neurocranium: With osteichthyans, there is a fundamental association (incorporation) between the premaxillary skeleton, derived from the FNP, and the mxBA1-derived maxillary and palatoquadrate skeletons (Fig. 1; detailed in Gregory, 1933; Schultze, 1993). The osteichthyan premaxillary arcade further develops in intimate association with the rostral neurocranium, in particular with the derivatives of the trabecular crainii and the nasal capsules, integrating and binding the BA derivatives with the rostral neurocranium and its associated dermatocranium. Generating an integrated upper jaw arcade, one involving integrated maxillary and premaxillary elements, necessitates coordinated frontonasal and mxBA1 development. Hence, it is reasonable to expect that such coordination would be reflected at some level in osteichthyan patterns of gene expression and not in chondrichthyan patterns.

Once established, maxillary–premaxillary–neurocranial osseous interconnectivity was central to a number of significant evolutionary transitions and radiations: For instance, making the maxillary–premaxillary–neurocranial connectivity less rigid and more movable enabled a distinct adaptive radiation in teleost (i.e., ray-finned fish such as the zebrafish) lineages (Gregory, 1933). Moreover, many of the most profound, propulsive gnathostome transitions involved elaborated development at the mxBA1–FNP connection, including both the acquisition of internal choanae enabling the colonization of land by tetrapods and the presence of a secondary palate, forming at the λ-junction, enabling mastication while breathing in the lineage leading to mammals (Fig. 1; see Halstead, 1968; Hildebrand, 1988; Kemp, 2005; Kingsley, 1912; Moore, 1981; Panchen, 1967; Rosen et al., 1981; Schmalhausen, 1968; Tamarin, 1982; Zhu and Ahlberg, 2004).

It is apodictic, then, that gaining greater understanding of jaw evolution, and the significant evolutionary transitions involving the jaws, requires further detailing which of the aspects of

gnathostome jaw development are shared within gnathostomes and which are derived and specific to a particular lineage, and then correlating molecular and genetic etiology with phenotypic end-product. Recognition, stemming from its posited importance in the 'Hinge and Caps' model, of the central importance of the λ-junction in craniofacial evolution has allowed us, for instance, to characterize a *Pbx-Wnt-p63-Irf6* regulatory module that correlates with the gradual increase in complexity of the mxBA1–FNP connection and associated structures (e.g., the choanae, upper lips and secondary palate) through evolutionary transitions from bony fish to mammals (Ferretti et al., 2011). Despite not possessing an elaborate mxBA1–FNP connection, chondrichthyans do exhibit clear 'Caps' associated gene expression patterns as predicted by the 'Hinge and Caps' model: Further investigation of the chondrichthyan maxillary 'Cap', therefore, will enable understanding of the evolution of the osteichthyan λ-junction.

Evidence of heterotopy as exemplified by Fgf8 expression

Gnathostome BAs therefore exhibit, in addition to a *Hox-Dlx* molecular construction, a well-conserved, basic 'cap-to-hinge-to-cap' architecture of gene expression along their proximo-distal axes. We found, however, a number of heterotopic patterns in gene expression. While we believe in the general caveat that each identified change in the timing and/or topography of the expression of a particular gene, whether seemingly minute or striking, must be further scrutinized and considered with more refined reference to homologous tissues and developmental staging – not necessarily a straight-forward endeavor – we also believe that some of the differences that we noted in gene expression between shark and amniote embryos will prove to be more profound than others. In particular, we believe that heterotopic differences between shark and amniote oral ectodermal expression of *Fgf8* – a secreted signaling factor with notable roles during development and a distinct cephalic expression pattern during ontogeny – is potentially significant (Fig. 8; Compagnucci et al., 2011; Crossley and Martin, 1995; Trumpp et al., 1999; Griffin et al., 2012). In both chick and mouse, *Fgf8* is expressed in the isthmus, ventro-lateral cephalic ectoderm, the olfactory pits, the pharyngeal plates and the hinge-centric oral ectoderm of both mxBA1 and mdBA1 (Fig. 8C and D). One notable difference between the chick and the mouse, however, is that murine *Fgf8* expression extends along the dorsal olfactory pit and spreads ventrally during ontogeny to eventually unite ventrally at the λ junction with the expression from the mxBA1 while that in the avian does not appear to. As with amniote embryos, *ScFgf8* is detected at the isthmus and in the ventro-lateral cephalic ectoderm, including in the dorsal olfactory pit (Fig. 8B and C). *ScFgf8* is also significantly expressed in the pharyngeal clefts: Strikingly, however, we failed to detect expression within the oral ectoderm of either mxBA1 or mdBA1 of the shark embryo at anytime point.

Using a *Cre*-mediated cephalic ectodermal conditional knockout, we previously demonstrated that loss of *Fgf8* in the oral ectoderm of the mouse is accompanied by catastrophic loss of the hinge region of the jaws (Trumpp et al., 1999). Notably, however, in these experiments the loss of *Fgf8* in the pharyngeal plate occurred slightly later and was correlated with the maintenance of a small population of cells at the pharyngeal cleft that gave rise to the malleus, the mammalian articular element homologue. Moreover, genetic attenuation of *Fgf8* dosage in mice leads to an associated disintegration of hinge structure and morphology (Griffin and Depew, in preparation). These and other studies have indicated that in amniotes, hinge-related *Fgf8* signaling is balanced between the epithelium of the oral ectoderm and that of the pharyngeal plate (Depew et al., 2002b; Depew and Compagnuicci, 2008). Moreover, *Fgf8* cognate expression in the lamprey, in a position topographically akin to the oral ectoderm, has been hypothesized as part of a heterotopic shift during the transition of gnathostomes from agnathans (see discussion in Shigetani et al., 2000, 2002, and Kuratani, 2012). Thus, discerning the functional significance of the absence of *ScFgf8* in the oral ectoderm is conceivably profound with regard to our understanding jaw development and evolution.

Conclusions

At present, the non-amniote gnathostome most studied at any depth for its jaw development is the teleostean fish, *D. rerio* (the zebrafish). While the zebrafish has proven to be a model organism tractable to genetic manipulation, at least two caveats regarding aspects of zebrafish jaw development and evolution must be taken into consideration when appraising zebrafish data with an eye toward comparisons amongst gnathostomes. First, teleosts represent a highly diverse, speciose crown group amongst gnathostomes (Gregory, 1933). The importance of this is epitomized by the fact that the developmental consequences for the patterning of the jaws of the additional chromosomal duplications that characterize the teleost radiation are yet to be fully understood. Second, the zebrafish embryo is extremely small, especially the region generating the jaws, and it is conceivable that such miniaturization effects how patterning information is exchanged between developing tissues. This issue is especially important, for example, when considering the effective radius, or sphere of influence, of secreted signals and their associated buffering.

Focused comparisons between chondrichthyans and the osteichthyans clades, including both bony fish and tetrapods, is nonetheless essential and is now possible. The great similarities between shark and amniote BA patterning may be reflective of a shared ancestry; they may also be reflective of convergence in jaw patterning. For numerous reasons, including its more parsimonious nature, we favor the former interpretation. Further investigation of the genetic, molecular and cellular underpinnings of BA patterning in other, and more basal, osteichthyan fish in comparison to those evinced in chondrichthyan as well as tetrapodal organisms, will enable a fuller picture of which molecular characteristics are ancestral for gnathostomes and which are derived and specific for each clade.

In summary, the presence of clear caps-to-hinge-to-caps polarity in gene expression patterns in the shark embryo establishes a baseline molecular baüplan for BA-derived jaw development, and further validates the utility of the 'Hinge and Caps' model in comparative studies of jaw development and evolution. Moreover, the absence of an elaborated λ-junction in chondrichthyans makes the investigation of shark jaw development all the more important for purposes of comparing and understanding jaw development and evolution. Because the elaboration of structure and function associated with the junction of the mxBA1 and FNP have been integral to so many gnathostome radiations, further understanding the basal molecular baüplan informing jaw development, as represented by the shark, becomes essential.

Acknowlegments

The authors would like to thank the FR 2424 Marine Model Facility, Roscoff Marine Station, who provided dogfish eggs. EST sequences were obtained with the support of Genoscope, Evry, France. The Depew lab would also like to thank Mara Beo and Dingle (Ireland) Oceanworld. This work was supported by funding to M.J.D. from the Royal Society, the Dental Institute of King's College London, and Friends of Guy's Hospital. C.C. and J.G. were

funded by Marie Curie Early Training Fellowships (MEST-CT-2004-504025). J.L.F. was assisted by a HFSP Long Term Fellowship (LT 01061/2007-L). S.M. was funded by Région Centre, Région Bretagne (EVOVERT grant number 049755), National Research Agency (grant ANR-09-BLAN-026201), CNRS, Université d'Orléans and the Université Pierre et Marie Curie. M.C. benefited from a doctoral fellowship from CNRS.

Appendix A. Supplementary materials

Supplementary data associated with this article can be found in the online version at http://dx.doi.org/10.1016/j.ydbio.2013.02.022.

References

Abu-Issa, R., Smyth, G., Smoak, I., Yamamura, K., Meyers, E.N., 2002. Fgf8 is required for pharyngeal arch and cardiovascular development in the mouse. Development 129, 4613–4625.

Abzhanov, A., Protas, M., Grant, B.R., Grant, P.R., Tabin, C.J., 2004. Bmp4 and morphological variation of beaks in Drawin's finches. Science 305, 1462–1465.

Abzhanov, A., Tabin, C.J., 2004. Shh and Fgf8 act synergistically to drive cartilage outgrowth during cranial development. Dev. Biol. 273, 134–148.

Allin, E.F., Hopson, J.A., 1992. Evolution of the auditory system in synapsida (''mammal-like reptiles'' and primitive mammals) as seen in the fossil record. In: Webster, DB, Fay, RR, Popper, AN (Eds.), The Evolutionary Biology of Hearing, Eds. Springer-Verlag, New York, US, pp. 587–614.

Arnason, U., Gullberg, A., Janke, A., 2001. Molecular phylogenetics of gnathostomous (jawed) fishes: old bones, new cartilage. Zool. Scripta 30, 249–255.

Ashique, A.M., Fu, K., Richman, J.M., 2002. Endogenous bone morphogenetic proteins regulate outgrowth and epithelial survival during avian lip fusion. Development 129, 4647–4660.

Balfour, F.M., 1878. A Monograph on the Development of Elasmobranch Fishes. McMillan and Co, London.

Ballard, W.W., Mellinger, J., Lechenault, H., 1993. A series of normal stages for development of *Scyliorhinus canicula*, the lesser spotted dogfish (Chondrichthyes: Scylorhinidae). J. Exp. Zool. 267, 318–336.

Barghusen, H.R., Hopson, A., 1979. The endoskeleton: the comparative anatomy of the skull and visceral skeleton. In: Wake, M. (Ed.), Hyman's Comparative Anatomy. The University of Chicago Press, Chicago, US, pp. 265–326.

Barlow, A.J., Francis-West, P.H., 1997. Ectopic application of recombinant BMP-2 and BMP-4 can change patterning of developing chick facial primordia. Development 124, 391–398.

de Beer, G.R., 1926. Studies on the vertebrate head. II. The orbito-temporal region of the skull. Q. J. Microsc. Sci. 278, 263–370.

de Beer, G.R., 1931. The development of the skull of scyllium (*Scyliorhinus canicula*) L. Q. J. Microsc. Sci. 74 591–564.

de Beer, G.R., 1985. The Development of the Vertebrate Skull. University of Chicago Press, Chicago, USA.

Bei, M., Mass, R., 1998. FGFs and BMP4 induce both Msx1-independent and Msx1-dependent signaling pathways in early tooth development. Development 125, 4325–4333.

Bell, E., Ensini, M., Gulisano, M., Lumsden, A., 2001. Dynamic domains of gene expression in the early avian forebrain. Dev. Biol. 236, 76–88.

Bellairs, A., Kamal, A.M., 1981. The chondrocranium and the development of the skull in recent reptiles. In: Morphology, C., Bellairs, A., Parsons, T.S. (Eds.), The Biology of the Reptilia, 11. Academic Press, London, UK.

Beverdam, A., Brouwer, A., Reijnen, M., Korving, J., Meijlink, F., 2001. Severe nasal clefting and abnormal embryonic apoptosis in Alx3/Alx4 double mutant mice. Development 128, 3975–3986.

Beverdam, A., Merlo, G.R., Paleari, L., Paleari, L., Mantero, S., Genova, F., Barbieri, O., Janvier, P., Levi, G., 2002. Jaw transformation with gain of symmetry after Dlx5/Dlx6 inactivation: mirror of the past? Genesis 34, 221–227.

Blentic, A., Panna, T., Payton, S., Walshe, J., Carney, T., Kelsh, R.N., Mason, I., Graham, A., 2008. The emergence of ectomesenchyme. Dev. Dyn. 237, 592–601.

Brickell, P., Thorogood, P., 1997. Retinoic acid and retinoic acid receptors in craniofacial development. Semin. Cell Dev. Biol. 8, 437–443.

Brazeau, M.D., Ahlberg, P.E., 2006. Tetrapod-like middle ear architecture in a Devonian fish. Nature 439, 318–321.

Brazeau, M.D., 2009. The braincase and jaws of a Devonian 'acanthodian' and modern gnathostome origins. Nature. 457, 305–308.

Bulfone, A., Kim, H.J., Puelles, L., Porteus, M.H., Grippo, J.F., Rubenstein, J.L., 1993. The mouse Dlx-2 (Tes-1) gene is expressed in spatially restricted domains of the forebrain, face and limbs in midgestation mouse embryos. Mech. Dev. 40, 129–140.

Carroll, R.L., 1988. Vertebrate Paleontology and Evolution. W. H. Freeman and Company, New York, USA.

Carroll, R.L., 1992. The primary radiation of terrestrial vertebrates. Annu. Rev. Ecol., Evol. Syst. 20, 45–84.

Cerny, R., Cattell, M., Sauka-Spengler, T., Bronner-Fraser, M., Yu, F., Meulemans Medeiros, D., 2010. Evidence for the prepattern/cooption model of vertebrate jaw evolution. PNAS 107, 17262–17267.

Chesterman, E.S., Kern, M.J., 2002. Comparative analysis of Prx1 and Prx2 expression in mice provides evidence for incomplete compensation. Anat. Rec. 266, 1–4.

Compagnucci, C., Fish, J.L., Schwark, M., Tarabyki, V., Depew, M.J., 2011. *Pax6* regulates craniofacial form through its control of an essential cephalic ectodermal patterning center. Genesis 49, 307–325.

Coolen, M., Menuet, A., Chassoux, D., Compagnucci, C., Henry, S., Lévèque, L., Da Silva, C., Gavory, F., Samain, S., Wincker, P., Thermes, C., D'Aubenton-Carafa, Y., Rodríguez-Moldes, I., Naylor, G., Depew, M., Sourdaine, P., Mazan, S., 2009. The dogfish *Scyliorhinus canicula*: a reference in jawed vertebrates. pp. 431–446. In: Behringer, R.R., Johnson, A.D., Krumlauf, R.E. (Eds.), Emerging Model Organisms. A Laboratory Manual, 1. Cold Spring Harbor Laboratory Press, New York, New York.

Coolen, M., Sauka-Spengler, T., Nicolle, D., Le-Mentec, C., Lallemand, Y., Da Silva, C., Plouhinec, J.L., Robert, B., Wincker, P., Shi, D.L., Mazan, S., 2007. Evolution of axis specification mechanisms in jawed vertebrates: insights from a chondrichthyan. PLoS One 2, e374.

Crossley, P.H., Martin, G.R., 1995. The mouse Fgf8 gene encodes a family of polypeptides and is expressed in regions that direct outgrowth and patterning in the developing embryo. Development 121, 439–451.

Cubbage, C.C., Mabee, P.M., 1996. Development of the cranium and paired fins in the zebrafish *Danio rerio* (*Ostariophysi*, *Cyprinadae*). J. Morphol. 229, 121–160.

Daniel, J.F., 1934. The Elasmobranch Fishes. University of California Press, Berkeley, USA.

Davis, S.P., Finarelli, J.A., Coates, M.I., 2012. Acanthodes and shark-like conditions in the last common ancestor of modern gnathostomes. Nature 486, 247–250.

Dean, B., 1909. Studies on fossil fish (Sharks, Chimaeroids and Arthrodires). Memoirs of the American Museum of Natural History IX, 211–287.

Debiais-Thibaud, M., Oulion, S., Bourrat, F., Laurenti, P., Casane, D., Borday-Birraux, V., 2011. The homology of odontodes in gnathostomes: insights from Dlx gene expression in the dogfish, *Scyliorhinus canicula*. BMC Evol. Biol. 11, 307.

Depew, M.J., 2008. Analysis of skeletal ontogenesis through differential staining of bone and cartilage. In: Sharpe, P.T., Mason, I. (Eds.), Molecular Embryology—Methods and Protocols. Humana Press, USA.

Depew, M.J., Compagnuicci, C., 2008. Tweaking the hinge and caps: testing a model of the organization of jaws. J. Exp. Zool. 310, 315–335.

Depew, M.J., Liu, J.K., Long, J.E., Presley, R., Meneses, J.J., Pedersen, R.A., Rubenstein, J.L., 1999. Dlx5 regulates regional development of the branchial arches and sensory capsules. Development 126, 3831–3846.

Depew, M.J., Lufkin, T., Rubenstein, J.L.R., 2002a. Specification of jaw subdivisions by Dlx genes. Science 298, 381–385.

Depew, M.J., Simpson, C.A., 2006. 21st century neontology and the comparative development of the vertebrate skull. Dev. Dyn. 235, 1256–1291.

Depew, M.J., Simpson, C.A., Morasso, M., Rubenstein, J.L., 2005. Reassessing the Dlx code: the genetic regulation of branchial arch skeletal pattern and development. J. Anat. 207, 501–561.

Depew, M.J., Tucker, A., Sharpe, P., 2002b. Craniofacial development. In: Rossant, J., Tam, P.P.L. (Eds.), Mouse Development: Patterning, Morphogenesis and Organogenesis. Academic Press, San Diego, USA, pp. 421–498.

Derobert, Y., Plouhinec, J.L., Sauka-Spengler, T., Le Mentec, C., Baratte, B., Jaillard, D., Mazan, S., 2002. Structure and expression of three Emx genes in the dogfish *Scyliorhinus canicula*: functional and evolutionary implications. Dev. Biol. 247, 390–404.

Didier, D.A., LeClair, E.E., Vanbuskirk, D.R., 1998. Embryonic staging and external features of development of the chimaeroid fish, *Callorhinchus milii* (*Holocephali*, Callorhinchidae). J. Morphol. 236, 25–47.

Dolle, P., Price, M., Duboule, D., 1992. Expression of the murine Dlx-1 homeobox gene during facial ocular and limb development. Differentiation 49, 93–99.

Dupe, V., Matt, N., Garnier, J.M., Chambon, P., Mark, M., Ghyselinck, N.B., 2003. A newborn lethal defect due to inactivation of retinaldehyde dehydrogenase type 3 is prevented by maternal retinoic acid treatment. PNAS 100, 14036–14041.

Ellies, D.L., Langille, R.M., Martin, C.C., Akimenko, M.A., Ekker, M., 1997a. Specific craniofacial cartilage dysmorphogenesis coincides with a loss of dlx gene expression in retinoic acid-treated zebrafish embryos. Mech. Dev. 61, 23–36.

Ellies, D.L., Stock, D.W., Hatch, G., Giroux, G., Weiss, K.M., Ekker, M., 1997b. Relationship between the genomic organization and the overlapping embryonic expression patterns of the zebrafish *dlx* genes. Genomics 45, 580–590.

El-Toubi, M.R., 1947. The development of the spiracular cartilages of the spiny dogfish, Acanthias vulgaris (*Squalus acanthias*). Biol Bull 93, 237–295.

El-Toubi, M.R., 1949. The development of the chondrocranium of the spiny dogfish, Acanthias vulgaris (*Squalus acanthias*) neurocranium, mandibular and hyoid arches. J. Morphol. 84, 227–279.

Evans, S.E., 2003. At the feet of the dinosaurs: the early history and radiation of lizards. Biol. Rev. 78, 513–551.

Ferreiro-Galve, S., Carrera, I., Candal, E., Villar-Cheda, B., Anadon, R., Mazan, S., Rodriguez-Moldes, I., 2008. The segmental organization of the developing shark brain based on neurochemical markers, with special attention to the prosencephalon. Brain Res. Bull. 75, 236–240.

Ferretti, E., Li, B., Zewdu, R., Wells, V., Hebert, J.M., Karner, C., Anderson, M.J., Williams, T., Dixon, J., Dixon, M.J., Depew, M.J., Selleri, L., 2011. A Conserved Pbx-Wnt-p63-Irf6 regulatory module controls face morphogenesis by promoting epithelial apoptosis. Dev. Cell 21, 627–641.

Fish, J.L., Villmoare, B., Köbernick, K., Compagnucci, C., Britanova, O., Tarabykin, V., Depew, M.J., 2011. Satb2, modularity, and the evolvability of the vertebrate jaw. Evol. Dev. 13, 549–564.
Foppiano, S., Hu, D., Marcucio, R.S., 2007. Signaling by bone morphogenetic proteins directs formation of an ectodermal signaling center that regulates craniofacial development. Dev. Biol. 312, 103–114.
Forey, P., Janvier, P., 1993. Agnathans and the origin of jawed vertebrates. Nature 361, 129–134.
Francis-West, P.H., Robson, L., Evans, D.J., 2003. Craniofacial development: the tissue and molecular interactions that control development of the head. Adv. Anat. Embryol. Cell Biol. 169, 1–138.
Freitas, R., Cohn, M.J., 2004. Analysis of EphA4 in the lesser spotted catshark identifies a primitive gnathostome expression pattern and reveals co-option during evolution of shark-specific morphology. Dev. Gene. Evol. 214, 466–472.
Freitas, R., Zhang, G., Cohn, M.J., 2006. Evidence that mechanisms of fin development evolved in the midline of early vertebrates. Nature 442, 1033–1037.
Freitas, R., Zhang, G., Cohn, M.J., 2007. Biphasic Hoxd gene expression in shark paired fins reveals an ancient origin of the distal limb domain. PLoS One 2, e754.
Furuta, Y., Hogan, B.L.M., 1998. BMP4 is essential for lens induction in the mouse embryo. Gene. Dev. 12, 3764–3775.
Gai, Z., Donoghue, P.C., Zhu, M., Janvier, P., Stampanoni, M., 2011. Fossil jawless fish from China foreshadows early jawed vertebrate anatomy. Nature 476, 324–327.
Gans, C., 1988. Craniofacial growth, evolutionary questions. Development 103, 3–15, Suppl.
Gans, C., Northcutt, R.G., 1983. Neural crest and origin of vertebrates: a new head. Science 220, 268–274.
Germot, A., Lecointre, G., Plouhinec, J.L., Le Mentec, C., Girardot, F., Mazan, S., 2001. Structural evolution of Otx genes in craniates. Mol. Biol. Evol. 18, 1668–1678.
Ghanem, N., Jarinova, O., Amores, A., Long, Q., Hatch, G., Park, B.K., Rubenstein, J.L., Ekker, M., 2003. Regulatory roles of conserved intergenic domains in vertebrate Dlx bigene clusters. Genome Res. 13, 533–543.
Gillis, J.A., Dahn, R.D., Shubin, N.H., 2009a. Shared developmental mechanisms pattern the gill arch and paired fin skeleton of vertebrates. PNAS 106, 5720–5724.
Gillis, J.A., Dahn, R.D., Shubin, N.H., 2009b. Chondrogenesis and homology of the visceral skeleton in the little skate, Leucoraja erinacea (Chondrichthyes: Batoidea). J. Morphol. 270, 628–643.
Gillis, J.A., Rawlinson, K.A., Bell, J., Lyon, W.S., Baker, C.V., Shubin, N.H., 2011. Holocephalan embryos provide evidence for gill arch appendage reduction and opercular evolution in cartilaginous fishes. Proc. Nat. Acad. Sci. U.S.A. 108, 1507–1512.
Godard, B.G., Mazan, S. 2012. Early patterning in a chondrichthyan model, the small spotted dogfish: towards the gnathosotme ancestral state. J. Anat. http://dx.doi.org/10.1111/j.1469-7580.2012.01552.x.
Goodrich, E.S., 1909. Vertebrata craniata (first fascicle: cyclostomes and fishes). In: Lankester, R. (Ed.), Treatise on Zollogy. Part IX. Adam and Charles Black, London.
Goodrich, E.S., 1918. On the development of the segments of the head in Scyllium. Q. J. Mic. Sci. 63, 1–30.
Goodrich, E.S., 1958. Studies on the Structure and Development of Vertebrates. Dover Publications, New York, USA.
Gong, S.G., Guo, C., 2003. Bmp4 gene is expressed at the putative site of fusion in the midfacial region. Differentiation 71, 228–236.
Gorski, J.A., Talley, T., Qiu, M., Puelles, L., Rubenstein, J.L., Jones, K.R., 2002. Cortical excitatory neurons and glia, but not GABAergic neurons, are produced in the Emx1-expressing lineage. J. Neurosci. 22, 6309–6314.
Gregory, W.K., 1933. Fish skulls: a study of the evolution of natural mechanisms. Trans. Amer. Philos. Soc. 23, 75–481.
Griffin, J.N., Compagnucci, C., Hu, D., Fish, J., Klein, O., Marcucio, R., Depew, M.J., 2013. Fgf8 dosage determines midfacial integration and polarity within the nasal and optic capsules. Dev. Biol. 374, 185–197.
Grogan, E.D., Lund, R., Didier, D., 1999. Description of the chimaerid jaw and its phylogenetic origins. J. Morphol. 239, 45–59.
Halstead, L.B., 1968. The Pattern of Vertebrate Evolution. WH Freeman and Co, San Francisco, USA.
Hanken, J., Hall, B.K., 1993. Mechanisms of skull diversity and evolution. In: Haken, J., Hall, B.K. (Eds.), The Skull, Volume 3: Functional and Evolutionary Mechanisms, University of Chicago Press, Chicago, US, pp. 1–36.
Hanken, J., Thorogood, P., 1993. Evolution and development of the vertebrate skull. TREE 8, 9–15.
Harrison, F.W., 1996. Development of the cranium and paired fins in the zebrafish *Danio rerio* (*Ostariophysi*, *Cyprinadae*). J. Morphol. 229, 121–160.
Hildebrand, M., 1988. Analysis of Vertebrate Structure. John Wiley & Sons, Inc., Toronto, Canada.
Holmgren, N., 1940. Studies on the head of fishes—embryological, morphological, and phylogenetic researches: Part I: Development of the skull in sharks and rays. Acta Zool. 21, 51–267.
Holmgren, N., 1942. Studies on the head of fishes. An embryological, morphological and phylogenetical study: Part III: The phylogeny of elasmobranch fishes. Acta Zool. 23, 129–261.
Iglesias, S.P., Lecointre, G., Sellos, D.Y., 2005. Extensive paraphylies within sharks of the order *Carcharhiniformes* inferred from nuclear and mitochondrial genes. Mol. Phylogenet. Evol. 34, 569–583.
Janvier, P., 1993. Patterns of diversity in the skull of jawless fishes. In: Haken, J., Hall, B.K. (Eds.), Patterns of Structural and Systematic Diversity, 2. University of Chicago Press, Chicago, US, pp. 131–188, In: The Skull.
Janvier, P., 1996. Early Vertebrates. Oxford University Press, Oxford, UK.
Jarvik, E., 1980. Basic Structure and Evolution of Vertebrates. Academic Press, New York, USA.
Jollie, M.T., 1957. The head skeleton of the chicken and remarks on the anatomy of this region in other birds. J. Morphol. 100, 389–436.
Jollie, M., 1962. Chordate Morphology. Reinhold, New York, USA.
Jollie, M., 1971. Some developmental aspects of the head skeleton of the 35–37 mm *Squalus acanthias* foetus. J. Morphol. 133, 17–40.
Kemp, T.S., 2005. The Origin and Evolution of Mammals. Oxford University Press, Oxford, UK.
Kingsley, J.S., 1907. The Dogfish (Acanthias): An Elasmobranch. Henry Holt and Co.
Kingsley, J.S., 1912. Comparative Anatomy of Vertebrates. Blakiston's and Sons, Philedelphia, USA.
Kuraku, S., Takio, Y., Sugahara, F., Takechi, M., Kuratani, S., 2010. Evolution of oropharyngeal patterning mechanisms involving Dlx and endothelins in vertebrates. Dev. Biol. 341, 315–323.
Kuratani, S., 2004. Evolution of the vertebrate jaw: comparative embryology and molecular developmental biology reveal the factors behind evolutionary novelty. J. Anat. 205, 335–347.
Kuratani, S., 2005. Developmental studies of the lamprey and hierarchical evolutionary steps towards the acquisition of the jaw. J. Anat. 207, 489–499.
Kuratani, S., 2012. Evolution of the vertebrate jaw from developmental perspectives. Evol. Dev. 14, 76–92.
Kuratani, S., Adachi, N., Wada, N., Oisi, Y., Sugahara, F., 2012. Develomental and evolutionary significance of the mandibular arch and prechordal/premandibular cranium in vertebrates: revising the heterotopy scenario of gnathostome jaw evolution. J. Anat., http://dx.doi.org/10.1111/j.1469-7580.2012.01505.x.
Kuratani, S., Horigome, N., 2000. Developmental morphology of branchiomeric nerves in a cat shark, *Scyliorhinus* torazame, with special reference to rhombomeres, cephalic mesoderm, and distribution patterns of cephalic crest cells. Zool. Sci. 17, 893–909.
Langille, R.M., Hall, B.K., 1989. Developmental processes, developmental sequences and early vertebrate phylogeny. Biol. Rev. Cambridge Philos. Soc. 64, 73–91.
Lee, S.H., Fu, K.K., Hui, J.N., Richman, J.M., 2001. Noggin and retinoic acid transform the identity of avian facial prominences. Nature 414, 909–912.
Lettice, L., Hecksher-Sorensen, J., Hill, R., 2001. The role of Bapx1 (Nkx3.2) in the development and evolution of the axial skeleton. J. Anat. 199, 181–187.
Liu, W., Selever, J., Murali, D., Sun, X., Brugger, S.M., Ma, L., Schwartz, R.J., Maxson, R., Furuta, Y., Martin, J.F., 2005a. Threshold-specific requirements for Bmp4 in mandibular development. Dev. Biol. 283, 282–293.
Liu, W., Sun, X., Braut, A., Mishina, Y., Behringer, R.R., Mina, M., Martin, J.F., 2005b. Distinct functions for Bmp signaling in lip and palate fusion in mice. Development 132, 1453–1461.
Maisey, J.G., 2001. Remarks on the inner ear of elasmobranchs and its interpretation from skeletal labyrinth morphology. J. Morphol. 250, 236–264.
Maisey, J.G., 2008. The postorbital palatoquadrate articulation in elasmobranchs. J. Morphol. 269, 1022–1040.
Mallatt, J., 1997. Crossing a major morphological boundary: the origin of jaws in vertebrates. Zoology 100, 128–140.
Matsuo, I., Kuratani, S., Kimura, C., Takeda, N., Aizawa, S., 1995. Mouse Otx2 functions in the formation and patterning of rostral head. Genes Dev. 9, 2646–2658.
McGonnell, I.M., Graham, A., Richardson, J., Fish, J.L., Depew, M.J., Dee, C.T., Holland, P.W.H., Takahashie, T., 2011. Evolution of the Alx homeobox gene family: parallel retention and independent loss of the vertebrate Alx3 gene. Evol. Dev. 13, 343–351.
Medeiros, D.M., Crump, J.G. 2012. New perspectives on pharyngeal dorsoventral patterning in development and evolution of the vertebrate jaw. Dev. Biol. 371, 121–135.
Meyer, A., Zardoya, R., 2003. Recent Advances in the (molecular) phylogeny of vertebrates. Annu. Rev. Ecol. Evol. Syst. 34, 311–338.
Mihailescua, D., Kury, P., Monard, D., 1999. An octamer-binding site is crucial for the activity of an enhancer active at the embryonic met-/mesencephalic junction. Mech. Dev. 84, 55–67.
Miles, R.S., 1964. A reinterpretation of the visceral skeleton of Acanthodes. Nature 204, 457–459.
Miller, C.T., Yelon, D., Stainier, D.Y.R., Kimmel, C.B., 2003. Two endothelin 1 effectors, hand2 and bapx1, pattern ventral pharyngeal cartilage and the jaw joint. Development 130, 1353–1365.
Minoux, M., Rijli, F.M., 2010. Molecular mechanisms of cranial neural crest cell migration and patterning in craniofacial development. Development 137, 2605–2621.
Moore, W.J., 1981. The Mammalian Skull. Cambridge University Press, Cambridge, UK.
Moy-Thomas, J.A., Miles, R.S., 1971. Palaeozoic fishes. W. B. Saunders and Co. Philadelphia, US.
Mulley, J.F., Zhong, Y.-F., Holland, P.W.H., 2009. Comparative genomics of chondrichthyan Hoxa clusters. BMC Evol. Biol. 9, 218.
Myojin, M., Ueki, T., Sugahra, F., Murakami, Y., Shigetani, Y., Aizawa, S., Hirano, S., Kuratani, S., 2001. Isolation of Dlx and Emx gene cognates in an Agnathan species, *Lampetra japonica*, and their expression patterns during embryonic and larval development: conserved and diversified regulatory patterns of

homeobox genes in vertebrate head evolution. J. Exp. Zool. (Mol. Dev. Evol.) 291, 68–84.
Neidert, A.H., Virupannavar, V., Hooker, G.W., Langeland, J.A., 2001. Lamprey *Dlx* genes and early vertebrate evolution. PNAS 98, 1665–1670.
Nelsen, O.E., 1953. Comparative Embryology of the Vertebrates. Blakiston Co, New York, USA.
Neubüser, A., Peters, H., Balling, R., Martin, G.R., 1997. Antagonistic interactions between FGF and BMP signaling pathways: a mechanism for positioning the sites of tooth formation. Cell 90, 247–255.
Novacek, M., 1993. Patterns of diversity in the mammalian skull. In: Haken, J., Hall, B.K. (Eds.), The Skull, Volume 2: Patterns of Structural and Systematic Diversity, University of Chicago Press, Chicago, US, pp. 438–545.
O'Neill, P., McCole, R.B., Baker, C.V.H., 2007. A molecular analysis of neurogenic placode and cranial sensory ganglion development in the shark, *Scyliorhinus canicula*. Dev. Biol. 304, 156–181.
Oulion, S., Borday-Birraux, V., Debiais-Thibaud, M., Mazan, S., Laurenti, P., Casane, D., 2011. Evolution of repeated structures along the body axis of jawed vertebrates, insights from the *Scyliorhinus canicula* Hox code. Evol. Dev. 13, 247–259.
Panchen, A.L., 1967. The nostrils of choanate fishes and early tetrapods. Biol. Rev. 42, 374–420.
Panganiban, G., Rubenstein, J.L., 2002. Developmental functions of the distal-less/Dlx homeobox genes. Development 129, 4371–4386.
Parrington, F.R., 1940. On the evolution of the human palate. Philos. Trans. R. Soc. London 230, 305–355.
Plouhinec, J.L., Leconte, L., Sauka-Spengler, T., Bovolenta, P., Mazan, S., Saule, S., 2005. Comparative analysis of gnathostome Otx gene expression patterns in the developing eye: implications for the functional evolution of the multigene family. Dev. Biol. 278, 560–575.
Qiu, M., Bulfone, A., Ghattas, I., Meneses, J.J., Christensen, L., Sharpe, P.T., Presley, R., Pedersen, R.A., Rubenstein, J.L., 1997. Role of the Dlx homeobox genes in proximodistal patterning of the branchial arches: mutations of Dlx-1, Dlx-2, and Dlx-1 and -2 alter morphogenesis of proximal skeletal and soft tissue structures derived from the first and second arches. Dev. Biol. 185, 165–184.
Qiu, M., Bulfone, A., Martinez, S., Meneses, J.J., Shimamura, K., Pedersen, R.A., Rubenstein, J.L., 1995. Null mutation of Dlx-2 results in abnormal morphogenesis of proximal first and second branchial arch derivatives and abnormal differentiation in the forebrain. Genes Dev. 9, 2523–2538.
Qu, S., Tucker, S.C., Ehrlich, J.S., Levorse, J.M., Flaherty, L.A., Wisdom, R., Vogt, T.F., 1998. Mutations in mouse aristaless-like4 cause strong's luxoid polydactyly. Development 126, 359–369.
Qu, S., Tucker, S.C., Zhao, Q., deCrombrugghe, B., Wisdom, R., 1999. Physical and genetic interactions between Alx4 and Cart1. Development 126, 359–369.
Radinsky, L.B., 1987. The Evolution of Vertebrate Design. University of Chicago Press, Chicago.
Ravi, V., Lam, K., Tay, B.H., Tay, A., Brenner, S., Venkatesh, B., 2009. Elephant shark (*Callorhinchus milii*) provides insights into the evolution of Hox gene clusters in gnathostomes. PNAS 106, 16327–16332.
Reif, W.E., 1980. Development of dentition and dermal skeleton in embryonic *Scyliorhinus canicula*. J. Morphol. 166, 275–288.
Rieppel, O., 1993. Patterns of diversity in the reptilian skull. In: Haken, J., Hall, B.K. (Eds.), Patterns of Structural and Systematic Diversity, 2. University of Chicago Press, Chicago, US, pp. 344–390, In: The Skull.
Renz, A.J., Gunter, H.M., Fischer, J.M.F., Qiu, H., Meyer, A., Kuraku, S., 2011. Ancestral and derived attributes of the dlx gene repertoire, cluster structure and expression patterns in an African cichlid fish. EvoDevo 2, 1–14.
Reynolds, S.H., 1913. The Vertebrate Skeleton. Cambridge University Press, Cambridge, US.
Rijli, F.M., Mark, M., Lakkaraju, S., Dierich, A., Dollé, P., Chambon, P., 1993. A homeotic transformation is generated in the rostral branchial region of the head by disruption of Hoxa-2, which acts as a selector gene. Cell 75, 1333–1349.
Robinson, G.W., Mahon, K.A., 1994. Differential and overlapping expression domains of Dlx-2 and Dlx-3 suggest distinct roles for Distal-less homeobox genes in craniofacial development. Mech. Dev. 48, 199–215.
Rodriguez-Moldes, I., Carrera, I., Pose-Mendez, S., Quintana-Urzainqui, I., Candal, E., Anadon, R., Mazan, S., Ferreiro-Galve, S., 2011. Regionalization of the shark hindbrain: a survey of an ancestral organization. Front. Neuroanat. 5, 16.
Romanoff, A.L., 1960. The Avian Embryo: Structural and Functional Development. MacMillan, New York, US.
Romer, A.S., 1966. Vertebrate Paleontology. University of Chicago Press, Chicago, USA.
Romer, A.S., 1967. Major steps in vertebrate evolution. Science 158, 1629–1637.
Rosen, D.E., Forey, P.L., Gardiner, B.G., Patterson, C., 1981. Lungfishes, tetrapods, paleontology, and plesiomorphy. Bull. Am. Mus.Nat. His. 167, 159–276.
Sakamoto, K., Onimaru, K., Munakata, K., Suda, N., Tamura, M., Ochi, H., Tanaka, M., 2009. Heterochronic shift in Hox-mediated activation of sonic hedgehog leads to morphological changes during fin development. PLoS One 4, e5121.
Santagati, F., Minoux, M., Ren, S.-Y., Rijli, F.M., 2005. Temporal requirement of Hoxa2 in cranial neural crest skeletal morphogenesis. Development 132, 4927–4936.
Satokata, I., Maas, R., 1994. Msx1 deficient mice exhibit cleft palate and abnormalities of craniofacial and tooth development. Nat. Genet. 6, 348–356.
Schaeffer, B., Williams, M., 1977. Relationships of fossil and living elasmobranchs. Am. Zool. 17, 293–302.
Schmalhausen, I.I., 1968. The Origin of Terrestrial Vertebrates. Academic Press, New York.
Schultze, H.P., 1993. Patterns of diversity in the skulls of jawed fishes. In: Haken, J., Hall, B.K. (Eds.), Patterns of Structural and Systematic Diversity, 2. University of Chicago Press, Chicago, US, pp. 189–254, In: The Skull.
Selleri, L., Depew, M.J., Jacobs, Y., Chanda, S.K., Tsang, K.Y., Cheah, K.S.E., Rubenstein, J.L.R., O'Gorman, S., Cleary, M.L., 2001. Requirement for *Pbx1* in skeletal patterning and programming chondrocyte proliferation and differentiation. Development 128, 3543–3557.
Shigetani, Y., Nobusada, Y., Kuratani, S., 2000. Ectodermally derived FGF8 defines the maxillomandibular region in the early chick embryo: epithelial-mesenchymal interactions in the specification of the craniofacial ectomesenchyme. Dev. Biol. 228, 73–85.
Shigetani, Y., Sugahara, F., Kawakami, Y., Murakami, Y., Hirano, S., Kuratani, S., 2002. Heterotopic shift of epithelial-mesenchymal interactions in vertebrate jaw evolution. Science 296, 1316–1319.
Shimeld, S.M., Holland, P.W., 2000. Vertebrate innovations. PNAS 97, 4449–4452.
Smith, K.K., 1993. The form of the feeding apparatus in terrestrial vertebrates: studies of adaptation and constraint. In: Haken, J., Hall, B.K. (Eds.), The Skull, Volume 3: Functional and Evolutionary Mechanisms, University of Chicago Press, Chicago, US, pp. 150–196.
Smith, M.M., Fraser, G.J., Chaplin, N., Hobbs, C., Graham, A., 2009. Reiterative pattern of sonic hedgehog expression in the catshark dentition reveals a phylogenetic template for jawed vertebrates. Proc. Biol. Sci. 276, 1225–1233.
Song, Y., Hui, J.N., Fu, K.K., Richman, J.M., 2004. Control of retinoic acid synthesis and FGF expression in the nasal pit is required to pattern the craniofacial skeleton. Dev. Biol. 276, 313–329.
Stock, D.W., 2005. The Dlx gene complement of the leopard shark, Triakis semifasciata, resembles that of mammals: implications for genomic and morphological evolution of jawed vertebrates. Genetics 169, 807–817.
Stock, D.W., Ellies, D.L., Zhao, Z., Ekker, M., Ruddle, F.H., Weiss, K.M., 1996. The evolution of the vertebrate Dlx gene family. Proc. Nat. Acad. Sci. 93, 10858–10863.
Sumiyama, K., Ruddle, F.H., 2003. Regulation of Dlx3 gene expression in visceral arches by evolutionarily conserved enhancer elements. Proc. Nat. Acad. Sci. U.S.A. 100, 4030–4034.
Szabo-Rogers, H.L., Geetha-Loganathan, P., Nimmagadda, S., Fu, K.K., Richman, J.M., 2008. FGF signals from the nasal pit are necessary for normal facial morphogenesis. Dev. Biol. 318, 289–302.
Talbot, J.C., Johnson, S.L., Kimmel, C.B., 2010. hand2 and Dlx genes specify dorsal, intermediate and ventral domains within zebrafish pharyngeal arches. Development 137, 2507–2517.
Tamarin, A., 1982. The formation of the primitive choanae and the junction of the primary and secondary palates in the mouse. Am. J. Anat. 165, 319–337.
Tamarin, A., Boyde, A., 1977. Facial and visceral arch development in the mouse embryo: a study by scanning electron microscopy. J. Anat. 124, 563–580.
Tavares, A.L.P., Garcia, E.L., Kuhn, K., Woods, C.M., Williams, T., Clouthier, D.E. 2012. Ectodermal-derived Endothelin1 is required for patterning the distal and intermediate domains of the mouse mandibular arch. Dev. Biol. 371, 47–56.
ten Berge, D., Brouwer, A., Korving, J., Martin, J.F., Meijlink, F., 1998. Prx1 and Prx2 in skeletogenesis: roles in the craniofacial region, inner ear and limbs. Development 125, 3831–3842.
Thomas, T., Kurihara, H., Yamagishi, H., Kurihara, Y., Yazaki, Y., Olson, E.N., Srivastava, D., 1998. A signaling cascade involving endothelin-1, dHAND and msx1 regulates development of neural-crest-derived branchial arch mesenchyme. Development 125, 3005–3014.
Trueb, L., 1993. Patterns of cranial diversity among the *Lissamphibia*. In: Haken, J., Hall, B.K. (Eds.), The Skull, Volume 2: Patterns of Structural and Systematic Diversity, University of Chicago Press, Chicago, US, pp. 255–343.
Trumpp, A., Depew, M.J., Rubenstein, J.L., Bishop, J.M., Martin, G.R., 1999. Cre-mediated gene inactivation demonstrates that FGF8 is required for cell survival and patterning of the first branchial arch. Genes Dev. 13, 3136–3148.
Tucker, A.S., Yamada, G., Grigoriou, M., Pachnis, V., Sharpe, P.T., 1999. Fgf-8 determines rostral-caudal polarity in the first branchial arch. Development 126, 51–61.
Tucker, A.S., Watson, R.P., Lettice, L.A., Yamada, G., Hill, R.E, 2004. Bapx1 regulates patterning in the middle ear: altered regulatory rolein the transition from the proximal jaw during vertebrate evolution. Development 131, 1235–1245.
Twigg, S.R., Versnel, S.L., Nürnberg, G., Lees, M.M., Bhat, M., Hammond, P., Hennekam, R.C., Hoogeboom, A.J., Hurst, J.A., Johnson, D., Robinson, A.A., Scambler, P.J., Gerrelli, D., Nürnberg, P., Mathijssen, I.M., Wilkie, A.O., 2009. Frontorhiny, a distinctive presentation of fronto- nasal dysplasia caused by recessive mutations in the ALX3 homeobox gene. Am. J. Hum. Genet. 84, 698–705.
Walker, M.B., Miller, C.T., Coffin Talbot, J., Stock, D.W., Kimmel, C.B., 2006. Zebrafish furin mutants reveal intricacies in regulating Endothelin1 signaling in craniofacial patterning. Dev. Biol. 295, 194–205.
Wall, N.A., Hogan, B.L., 1995. Expression of bone morphogenetic protein-4 (BMP-4), bone morphogenetic protein-7 (BMP-7), fibroblast growth factor-8 (FGF-8) and Sonic hedgehog (SHH) during branchial arch development in the chick. Mech. Dev. 53, 383–392.
Watson, D.M.S, 1926. Croonian lecture: the evolution and origin of the amphibia. Philos. Trans. R. Soc. London 214, 189–257.
Watson, D.M.S., 1937. The aconthodian fishes. Philos. Trans. R. Soc. London, Ser. B 228, 49–146.

Wilga, C.D., 2002. A functional analysis of jaw suspension in elasmobranchs. Biol. J. Linn. Soc. 75, 483–502.
Williams, J.A., Mann, F.M., Brown, N.A. 1997. Gene expression domains as markers in developmental toxicity studies using mammalian embryo culture. Int. J. Dev. Biol. 41, 359–364.
Wotton, K.R., Mazet, F., Shimeld, S.M., 2008. Expression of FoxC, FoxF, FoxL1, and FoxQ1 genes in the dogfish *Scyliorhinus canicula* defines ancient and derived roles for Fox genes in vertebrate development. Dev Dyn. 237, 1590–1603.
Wu, P., Jiang, T., Suksaweang, S., Widelitz, R.B., Chuong, C.M., 2004. Molecular shaping of the beak. Science 305, 1465–1466.
Yanagisawa, H., Hammer, R.E., Richardson, J.A., Emoto, N., Williams, S.C., Takeda, S., Clouthier, D.E., Yanagisawa, M., 2000. Disruption of ECE-1 and ECE-2 reveals a role for endothelin-converting enzyme-2 in murine cardiac development. J. Clin. Invest. 105, 1373–1382.
Young, J.Z., 1981. The Life of Vertebrates. Oxford University Press, Oxford, UK.
Zhu, M., Ahlberg, P.E., 2004. The origin of the internal nostril of tetrapods. Nature 432, 94–97.
Zirzowa, S., Lüdtkea, T.H.W., Bronsb, J.F., Petrya, M., Christoffelsb, V.M., Kispert, A., 2009. Expression and requirement of T-box transcription factors Tbx2 and Tbx3 during secondary palate development in the mouse. Dev. Biol. 336, 145–155.
Zusi, R.L., 1993. Patterns of diversity in the avian skull. In: Haken, J., Hall, B.K. (Eds.), The Skull, Volume 2: Patterns of Structural and Systematic Diversity, University of Chicago Press, Chicago, US, pp. 391–437.